Macromolecules 2006, *39*, 2284−2290

Protein Repellency of Well-Defined, Concentrated Poly(2-hydroxyethyl methacrylate) Brushes by the Size-Exclusion Effect

Chiaki Yoshikawa,† Atsushi Goto,† Yoshinobu Tsujii,† Takeshi Fukuda,*,† Tsuyoshi Kimura,§ Kazuya Yamamoto,‡ and Akio Kishida§

Institute for Chemical Research, Kyoto University, Uji, Kyoto 611-0011, Japan; Department of Nanostructured and Advanced Materials, Graduate School of Science and Engineering, Kagoshima University, 1-21140 Korimoto, Kagoshima 890-0065, Japan; and Institute of Biomaterials and Bioengineering, Tokyo Medical and Dental University, Chiyoda, Tokyo 101-0062, Japan

Received September 17, 2005; Revised Manuscript Received November 10, 2005

ABSTRACT: The adsorption of proteins on poly(2-hydroxyethyl methacrylate) (PHEMA) brushes was systematically studied by quartz crystal microbalance (QCM) and fluorescence microscopy as a function of graft density and protein size. The graft density σ (chains/nm^2) ranged from 0.007 (dilute or semidilute brush regime) to 0.7 (concentrated brush regime), and the protein size ranged from 2 to 13 nm in an effective diameter. The lowest-density brush ($\sigma = 0.007$) adsorbed all the tested four proteins, while the highest-density brush ($\sigma = 0.7$) adsorbed none of them. The middle-density brush ($\sigma = 0.06$) showed an intermediate behavior, adsorbing the smallest two proteins but effectively repelling the largest two. PHEMA cast films adsorbed a probe protein with the adsorbed amount increasing approximately proportionally to the film thickness, indicating that the adsorption mainly occurred in the bulk of the film. The noted results for the brushes support the idea of size-exclusion effect, an effect characteristic of concentrated polymer brushes, in which the graft chains are highly extended and highly oriented so that large molecules, sufficiently large compared with the distance between the nearest-neighbor graft points, are *physically* excluded from the entire brush layer. In this regard, the behavior of the lowest-density brush should be essentially similar to that of the cast film, as was in fact observed.

Introduction

Living radical polymerization (LRP) has been applied to surface-initiated graft polymerization, allowing controlled grafting of well-defined polymers from various solid surfaces with dramatically high surface densities.[1−9] The surface density σ reached as large as 0.7 chains/nm^2 for common polymers like poly(methyl methacrylate) (PMMA) and polystyrene (PS).[9] This density was more than 1 order of magnitude higher than those of typical "semidilute" brushes, going deep into the "concentrated brush" regime which had been little explored systematically because of the unavailability of such brush samples. Recent studies revealed that these concentrated brushes have structure and properties quite different and even unpredictable from those of semidilute brushes:[9] most strikingly, the PMMA concentrated brushes swollen in a good solvent (toluene) exhibited an equilibrium film thickness as large as 80−90% of the full (contour) length of the graft chains, indicating that the chains are extended to a similarly high degree.[9,10] The surface density of 0.7 chains/nm^2 for a PMMA brush, for example, also means that the thickness of the dry film reaches about 40% of the full length of the chains, which is much larger than the mean size of the chains in a random-coil (or so-called "mushroom") conformation. Presumably reflecting this characteristic conformational feature of concentrated brushes, dry PMMA brushes had a glass transition temperature significantly higher,[11] and a plate compressibility markedly smaller,[12] than those of the equivalent cast films. More interestingly, they were immiscible even with free PMMA of an oligomeric chain length.[9,13] This last observation suggests that concentrated brushes in the melt have a size-exclusion effect of (conformational) entropic origin. A similar effect is expectable for concentrated brushes swollen in a good solvent, as, in fact, was demonstrated chromatographically by using the silica monolith column coated with concentrated PMMA brushes.[9,14]

As one of the most interesting potential applications of polymer brushes, attention has been directed toward biointerfaces to tune interactions of solid surfaces with biologically important materials. For example, proteins will adsorb on surfaces through nonspecific interactions, often triggering a biofouling, e.g., the deposition of biological cells, bacteria, and so on. Attempts have been made to modify surfaces with polymer brushes to prevent protein adsorption. To understand the process of protein adsorption, the interactions between proteins and brush-coated surfaces can be modeled by the three generic modes illustrated in Scheme 1a (after Curie et al.[15] with some modifications). One is the primary adsorption, in which a protein diffuses into the brush and adsorbs on the substrate surface. The secondary adsorption is the one occurring at the outermost surface of the swollen brush film. The last one is the tertiary adsorption, which is caused by the interaction of protein with the polymer segments within the brush layer. For relatively small proteins, the primary and tertiary adsorptions would be particularly important, but they should become less important with increasing protein size and increasing graft density, since a larger protein would be more difficult to diffuse against the concentration gradient formed by the polymer brush, and this gradient, clearly, is a function of graft density. However, the size and density dependence of protein adsorption would manifest itself much more clearly for concentrated brushes due to a different mechanism. As already noted, the graft chains in

† Kyoto University.
‡ Kagoshima University.
§ Tokyo Medical and Dental University.
* Corresponding author: e-mail fukuda@scl.kyoto-u.ac.jp.

10.1021/ma0520242 CCC: $33.50
Published on Web 02/25/2006

Scheme 1. Schematic Illustration of (a) Possible Interactions of Probe Molecules with a Polymer Brush and (b) Size-Exclusion Effect of Concentrated Brush

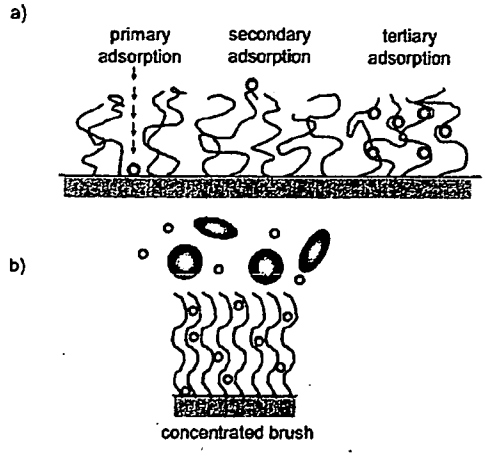

a concentrated brush are highly extended and hence highly oriented so that the entire brush layer, from the substrate surface to the outermost surface throughout, could have a size-exclusion effect (Scheme 1b). By the terms "size exclusion", we stress the *physical* aspect of the phenomenon, meaning that the protein (or probe molecule) is excluded from the brush layer to avoid the large (mainly conformational) entropy loss caused on the highly extended chains by the entrance of the large molecule. Since the degree of chain extension is much less significant in semidilute brushes, this effect should be minor for them.

In the past, poly(ethylene oxide) (PEO)-grafted surfaces were extensively studied to discuss their protein adsorption behavior as a function of graft density.[15-21] However, since those surfaces were prepared by physisorption of block copolymers or comb-like polymers using a self-assembling or the Langmuir–Blodgett technique, the graft density should have been in a semidilute regime, i.e., too low to observe the mentioned effect clearly, if any present. Well-defined concentrated brushes achievable by surface-initiated LRP would set up size-exclusion limits at much smaller sizes of probe molecules, thus allowing us to explore them with available proteins. Most recently, poly(acrylamide),[22] poly(2-(dimethylamino)ethyl methacrylate),[23] poly(oligo(ethylene glycol) methyl methacrylate),[24] and poly(2-methacryloxyethylphosphorylcholine) (PMPC)[25-27] brushes were prepared by surface-initiated LRP and observed to show good adsorption resistance for proteins and cells. From a mechanistic point of view, however, these studies remained purely qualitative, paying little attention to the mentioned characteristics of concentrated brushes.

In this work, we have attempted to substantiate the postulated size-exclusion effect of concentrated polymer brushes by systematically studying the adsorption behavior of varying sizes of proteins on the substrates grafted with a poly(2-hydroxyethyl methacrylate) (PHEMA) brush of varying surface densities, by means of quartz crystal microbalance (QCM) and fluorescence microscopy. PHEMA is a hydrophilic, biocompatible polymer,[28] but the biocompatibility of PHEMA cast film is reported to be not as good as e.g. PMPC[29,30] and poly(2-methoxyethyl acrylate) cast films.[31,32] Hence, any favorable results that PHEMA brushes may present could be ascribed more to the structural, rather than thermodynamic, properties of the system. Our ultimate goal is to develop, by utilizing the advantages of surface-initiated LRP,[9] a concentrated brush-based, new biointerface that will completely suppress the adsorption of small as well as large proteins. This work should be an important step for this goal.

Scheme 2. Schematic Illustration of Graft Polymerizations on an Inorganic Substrate: (a) Surface-Initiated ATRP and (b) a Grafting-To Method

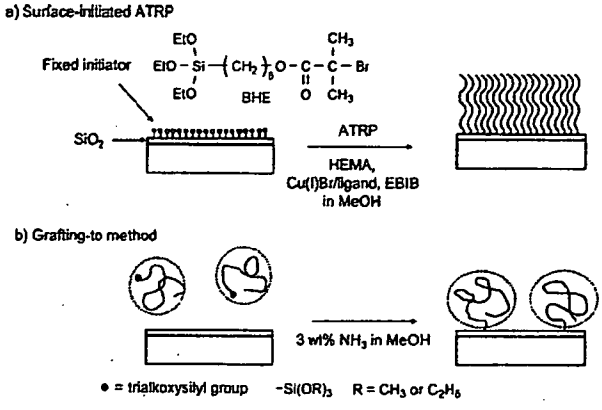

Experimental Section

Materials. 2-Hydroxyethyl methacrylate (HEMA) (99%, Nacalai Tesque, Japan) was purified according to the literature.[33] Cu(I)Br (99.9%, Wako Pure Chemical, Japan), ethyl 2-bromoisobutylate (EBIB) (99%, Wako), 2,2-bipyridine (bpy) (99%, Nacalai), methanol (99%, Nacalai), phosphate-buffered saline (PBS) (pH = 7.4, Wako), ammonia (28% aqueous, Nacalai), 3-mercaptopropyltrimethoxysilane (S810) (Chisso, Japan), and 2,2′-azobis(4-methoxy-2,4-dimethylvaleronitrile) (V70) (99.9%, Wako) were used as received. 6-(2-Bromo-2-isobutyloxy)hexyltriethoxysilane (BHE), a fixable initiator for ATRP, was prepared, as previously reported.[34] Bovine serum aprotinin (Aprotinin), bovine serum albumin (BSA), fluorescein isothiocyanate-labeled BSA (FITC-BSA), bovine serum immunoglobulin G (IgG), and horse heart myoglobin (Myoglobin) were purchased from Sigma-Aldrich and used as received.

Silicon wafers were cleaned by ultrasonication in $CHCl_3$ for 30 min and ultraviolet (UV)/ozone treatment for 10 min. The UV/ozone treatment effectively removed organic contaminants on the wafer surfaces. QCM chips (optically polished square-shaped AT-cut quartz crystals (1 × 1 cm²) with gold electrodes) (Seiko EG&G, Seiko Instruments Inc.) were similarly cleaned. On the cleaned chip, Cr and then SiO_2 were deposited in a vacuum with the thicknesses of 5 and 40 nm, respectively.

Preparation of High-Density Brushes (σ = 0.7 Chains/nm²). High-density PHEMA brushes were prepared by surface-initiated ATRP, as shown in Scheme 2a. A silicon wafer and a SiO_2-deposited QCM chip were immersed in a tetrahydrofuran (THF) solution of BHE (1 wt %) and NH_3 (1 wt %) for 12 h at room temperature and washed with THF. The BHE-immobilized substrate (wafer and chip) was immersed in a degassed methanol solution of HEMA (4.5 M), Cu(I)Br (25 mM), bpy (63 mM), and the free initiator EBIB (22.5 mM), sealed under vacuum in a glass tube (1 cm diameter), and heated at 40 °C for a prescribed time. This polymerization condition was referred to Armes et al., who successfully prepared low-polydispersity free polymers of HEMA.[35] After polymerization, the solution was diluted with *N,N*-dimethylformamide (DMF) to a known concentration and analyzed by gel permeation chromatography (GPC). The conversion was determined from the GPC peak area. The substrate was rinsed in a Soxhlet apparatus with methanol for 5 h to remove physisorbed free polymers and impurities.

Preparation of Middle- and Low-Density Brushes (σ = 0.06 and 0.007 Chains/nm²). Middle- and low-density PHEMA brushes were prepared by a grafting-to method, as shown in Scheme 2b. Namely, PHEMA chains with an alkoxysilyl group at one chain end were immobilized on a silicon wafer and a SiO_2-deposited QCM chip in solution. Two end-functionalized PHEMAs with different chain lengths were used. The shorter one (M_n = 9800 and M_w/M_n = 1.2) was synthesized by ATRP with BHE (with a triethoxysilyl group) used as a free initiator: a degassed methanol solution of HEMA (4.5 M), BHE (22.5 mM), Cu(I)Br (25 mM), and bpy (63

Table 1. Characteristics of Studied PHEMA Surfaces

surface[a]	$M_{n,conv}$[b]	$M_{n,PEG}$[c]	M_w/M_n[c]	L[d](nm)	σ[e](chain nm^{-2})	d[f](nm)	θ[g](deg)
high-density brush	1700	3500	1.21	2	0.7	1	29
high-density brush	9700	8000	1.26	10	0.7	1	
high-density brush	16800[h]	12300	1.30	15	0.7	1	29
middle-density brush	19000	15300	1.27	2	0.06	4	27
low-density brush		1.2×10^5	1.24	2	0.007[i]	12	29
cast film		$>4 \times 10^5$		30			23
cast film		$>4 \times 10^5$		90			23
cast film		$>4 \times 10^5$		330			23
BHE[j]							55

[a] Characteristics of brushes were almost identical on silicon wafers and QCM chips, and typical values on silicon wafers are listed. [b] Calculated according to eq 3. [c] Estimated by PEG-calibrated GPC. [d] Film thickness, the error is within 10%. [e] Graft density, calculated with L and $M_{n,conv}$ according to eq 2. [f] Average distance between the nearest-neighbor graft points, calculated according to $d = \sigma^{-1/2}$. [g] Contact angle; the error is within 2°. [h] The $M_{n,MALLS}$ is 17600 (see text). [i] Calculated with L and $M_{n,MALLS}$ (1.8×10^5) according to eq 2. [j] BHE-immobilized surface.

mM) was heated at 30 °C for 1 h. After reprecipitation with cooled water, there was isolated a PHEMA ($M_n = 1.5 \times 10^4$ and $M_w/M_n = 1.2$) possessing a triethoxysilyl group (derived from BHE) at one chain end. A silicon wafer and a SiO_2-deposited QCM chip were immersed in a methanol solution of the PHEMA (1 wt %) and NH_3 (2 wt %) for 12 h at room temperature and rinsed in a Soxhlet apparatus with methanol for 5 h, yielding a middle-density brush ($\sigma = 0.06$ chains/nm^2).

The longer end-functionalized PHEMA was prepared by the conventional radical polymerization with the chain transfer agent S810: a methanol solution of HEMA (4.5 M), S810 (chain transfer agent; 9 mM), and V70 (9 mM) was heated at 40 °C for 2 h. The obtained polymer was fractionated by use of a preparative GPC, yielding a PHEMA ($M_n = 1.2 \times 10^5$ and $M_w/M_n = 1.2$) possessing a trimethoxysilyl group (derived from S810) at one chain end. This polymer was immobilized on a silicon wafer and a SiO_2-deposited QCM chip as described above, yielding a low-density brush ($\sigma = 0.007$ chains/nm^2).

Preparation of Cast Films. PHEMA ($M_v = 10^6$) (Aldrich), after having purified by reprecipitation from a methalol solution into cold water, was dissolved in methanol. The cast films were obtained by spin-casting the PHEMA solution onto a silicon wafer using a homemade spin-coater at a spinning speed of 2000 rpm for 2 min, followed by annealing at 80 °C for 24 h in a vacuum. The film thickness was controlled by changing the concentration of PHEMA solution.

QCM Measurement. Protein adsorption was studied at 25 °C with a quartz crystal analyzer 917 (Seiko EG&G) driving a 9 MHz QCM chip. The QCM chip was mounted in a thermostated homemade QCM cell by means of O-ring seals, which allowed only one face of the chip to come in contact with the solution. Before injection of a PBS solution of a protein, the QCM cell was initially filled with PBS and rinsed several times until a stable baseline was established. The stability of the frequency of QCM was ±0.3 Hz within 1 h at 25 °C in water. The adsorbed amount Δm (ng) is represented by[36]

$$\Delta m = -\Delta f A((\mu_q \rho_q)/(2F_q^2))^{1/2} \quad (1)$$

where Δf is the frequency change (Hz), F_q is the parent frequency of QCM (9 MHz), μ_q is the shear modules of quartz (2.947×10^{11} g/(cm s^2)), ρ_q is the density of quartz (2.648 g/cm^3), and A is the surface area of electrode (0.196 cm^2).

Fluorescence Microscopic Observation. The sample was immersed in a PBS solution of FITC-BSA (1.0 g/L) for a prescribed time at room temperature. The sample was washed by softly immersing in PBS, and this procedure was repeated five times with fresh PBS. Fluorescence images were taken on an optical microscope (Eclipse TE2000, Nikon, Tokyo, Japan) equipped with a highly sensitive CCD camera (ORCA-ER, Hamamatsu Photonics, Shizuoka, Japan). The observation was made on at least five spots for each sample, and the fluorescence intensities of these spots were averaged. To check reproducibility of the FITC-BSA adsorption, at least three samples were prepared under the same conditions and examined.

Other Measurements. The GPC analysis for PHEMA was made on a Tosoh CCP&8020 series high-speed liquid chromatograph (Tokyo, Japan) equipped with two Shodex gel columns LF804 (300 × 80 mm; bead size = 6 μm; pore size = 20−3000 Å) (Tokyo). DMF was used as eluent with a flow rate of 0.8 mL/min (40 °C). The column system was calibrated with Tosoh standard poly(ethylene glycol)s (PEGs). Sample detection and quantification were made with a Tosoh differential refractometer RI-8020. Sample detection was also made with a multiangle laser light scattering (MALLS) detector, a Wyatt Technology DAWN EOS (Santa Barbara, CA), equipped with a Ga−As laser ($\lambda = 690$ nm). The refractive index increment dn/dc was determined to be 0.075 mL g^{-1} by a Wyatt Technology OPTILAB DSP differential refractometer ($\lambda = 690$ nm).

For the GPC analysis of proteins, the above-noted chromatograph equipped with a Shodex gel column KW804 (300 × 80 mm; bead size = 7 μm; pore size = 300 Å) (Tokyo) was calibrated with Shodex standard pullulans. PBS was used as eluent with a flow rate of 0.8 mL/min (30 °C).

The fractionation of PHEMA was made on a preparative LC-918 liquid chromatograph (Japan Analytical Industry, Tokyo) equipped with JAIGEL GS-510 poly(vinyl alcohol) gel columns (500 × 21.5 mm; bead size = 16 μm). Methanol was used as eluent with a flow rate of 5.0 mL/min (room temperature).

The thicknesses of the deposited Cr and SiO_2 and the grafted and spin-casted PHEMA layers were determined by a compensator-rotating, spectroscopic ellipsometer (M-2000U, J.A. Woolam, Lincoln, NE) equipped with D_2 and QTH lamps. The polarizer angle was 45°, and the incident angles were 60°, 65°, and 70°. From the ellipsometric data, the thickness of PHEMA layer was evaluated using the optical constants determined for the spin-cast layer with a thickness of ca. 200 nm. The graft density σ was estimated from

$$\sigma = L\rho N_A/M_n \quad (2)$$

where L is the thickness of graft layer, ρ is the bulk density of PHEMA (1.15 g/cm^3), N_A is the Avogadro number, and M_n is the number-average molecular weight.

Contact angles (θ) were measured at room temperature with a contact angle meter CA-X (Kyowa Interface Science, Saitama, Japan). The measurement was made on at least five spots for each sample, and these θ values were averaged.

Results and Discussion

Preparation and Characterization of PHEMA Brushes. The "high-density" PHEMA brushes were prepared by surface-initiated ATRP. A few previous reports dealt with surface-initiated LRP of HEMA,[37−39] but we made an independent effort to optimize polymerization conditions to meet our purpose. Three samples with different chain lengths of PHEMA (and hence, different thicknesses of the graft layer) were prepared by varying the polymerization time. Table 1 lists the M_n and M_w/M_n of the free polymers simultaneously produced from the free initiator in the solution. These values can be used as

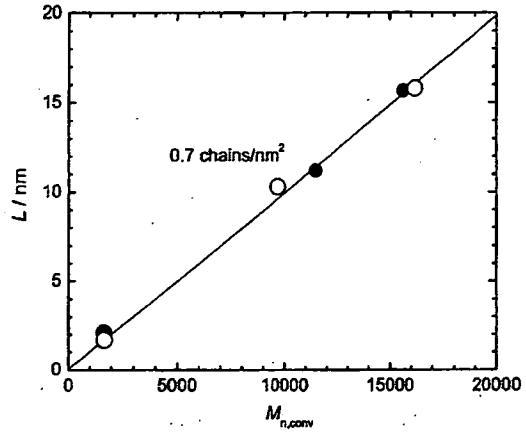

Figure 1. Plot of L vs $M_{n,conv}$ for the high-density brushes prepared on (●) silicon wafer and (○) QCM chip.

sufficiently accurate indices for those of the graft polymers.[4] The M_w/M_n was 1.2−1.3 in all cases, suggesting a well-controlled polymerization. The $M_{n,conv}$ was calculated using the following equation:

$$M_{n,conv} = [HEMA]_0/[EBIB]_0 \times MW \times C/100 \quad (3)$$

where $[HEMA]_0$ and $[EBIB]_0$ are the feed concentration of HEMA and EBIB, respectively, MW is the molecular weight of HEMA, and C is the monomer conversion in percent. This value is the theoretical M_n for an ideal living polymerization. To evaluate the absolute value of M_n, the GPC detection was made with a MALLS detector for the highest-molecular-weight sample (prepared by the ATRP): the thus-determined M_n ($M_{n,MALLS}$ = 17 600) agreed well with the theoretical value ($M_{n,conv}$ = 16 800) rather than the PEG-calibrated M_n ($M_{n,PEG}$ = 12 300). For the oligomeric PHEMAs prepared by nearly the same ATRP system, Armes et al. reported that the absolute M_n determined by NMR was approximately equal to the $M_{n,conv}$.[35] We will use $M_{n,conv}$ for the absolute value.

The thickness L of the graft layer measured by ellipsometry linearly increased with increasing $M_{n,conv}$ of the free polymer (see Figure 1), suggesting a uniform growth of graft polymer with a constant surface density. From the slope of the line in Figure 1, the graft density σ was estimated to be ca. 0.7 chains/nm², which is similar to the highest values reported for PMMA and PS brushes.[9] Brushes with lower graft densities were prepared by a grafting-to method using two end-functionalized PHEMAs with $M_n = 1.5 \times 10^4$ and 1.2×10^5. They gave the "middle-density" (σ = 0.06 chains/nm²) and "low-density" (σ = 0.007 chains/nm²) brushes, respectively. These PHEMA brushes can be grouped into two series: one series is the high-density brushes with a nearly constant graft density of 0.7 chains/nm² and different dry film thicknesses 2, 10, and 15 nm, and the other is the brushes with nearly the same dry film thickness of 2 nm and different graft densities 0.007, 0.06, and 0.7 chains/nm².

The contact angle θ was measured in water by the air-bubble method for these brushes as well as a BHE-immobilized wafer and three PHEMA spin-cast films of thicknesses 30, 90, and 330 nm (Table 1). The BHE-immobilized surface (nongrafted surface) was much more hydrophobic than the PHEMA-coated samples (brushes and cast films). The brushes had a θ value slightly (about 5°) higher than the cast films (the experimental error in θ was ±2°), for an unclear reason. The observed dependence (or independence) of θ on graft density and film thickness suggests that the substrate was completely covered

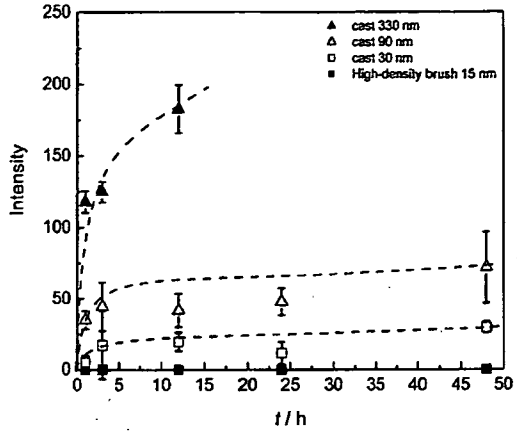

Figure 2. Plot of fluorescence intensity of adsorbed FITC-BSA vs soaked time t (25 °C) for the cast films with L = (▲) 330 nm, (△) 90 nm, and (□) 30 nm and the high-density brush with L = 15 nm (■). The FITC-BSA concentration was 1.0 g/L.

with PHEMA segments in all cases. The effect of the chain end (bromine for the high- and middle-density brushes and hydrogen for the low-density brush) is not evident even for the high-density brushes, in which, because of their oriented structure stressed above, the free chain ends and hence the bromine groups should be populated in the outermost surface of the film.

Adsorption of BSA. By fluorescence microscopy, we examined the adsorption of BSA on PHEMA cast film as a function of thickness: the cast films with different thicknesses (L = 30, 90, and 330 nm) prepared on silicon wafers were soaked in a FITC-BSA solution (1 g/L) at room temperature for a prescribed time, rinsed with PBS, and then observed by a fluorescence microscope. The fluorescence intensity was almost unchanged by further rinsing with PBS, confirming an irreversible adsorption. The fluorescence images suggested that BSA was homogeneously adsorbed (in an optical microscopic scale). Figure 2 shows the plot of fluorescence intensity vs soaked time. Unfortunately, the fluorescence intensity was not calibrated to the amount of adsorbed BSA, but the proportional relationship between them may reasonably be assumed. As a rough measure of the adsorbed amount, we may refer to the previous study reporting that 0.38 μg/cm² of BSA was adsorbed on PHEMA cast films.[32] The fluorescence intensity and hence the amount of adsorbed BSA gradually increased in several hours, approaching a constant (saturation) value. As Figure 3 shows, the intensity at 12 h, as a measure of the saturation value, increased almost proportionally to film thickness L. This means that BSA diffuses deeply into the bulk of the cast film, and that the adsorption in this system consists mainly of the tertiary adsorption with minor contributions of the primary and secondary ones. It naturally took a very long time to reach the saturation value (as compared with the case of high-density brush samples, for example, to be described below).

Next, we examined the adsorption of BSA on the brushes and the BHE-immobilized surfaces by QCM. This method allows in situ monitoring of the adsorption process with a usually high sensitivity. However, when it is applied to a viscoelastic layer in solution, the dissipation effect causes an error in estimating the mass according to eq 1. This error becomes larger with increasing layer thickness, and for this reason, our cast films were too thick to apply QCM. We confirmed that the QCMs with different fundamental frequencies (5 and 9 MHz) gave a consistent result for the brush samples with L = 10 nm or thinner, meaning that the dissipation effect was minor for

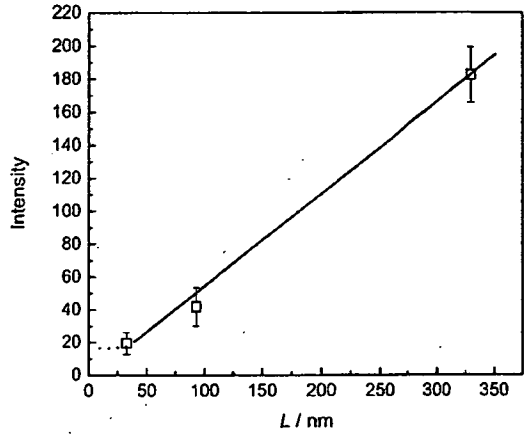

Figure 3. Plot of intensity of adsorbed FITC-BSA vs L for the cast films soaked for 12 h (25 °C). The FITC-BSA concentration was 1.0 g/L.

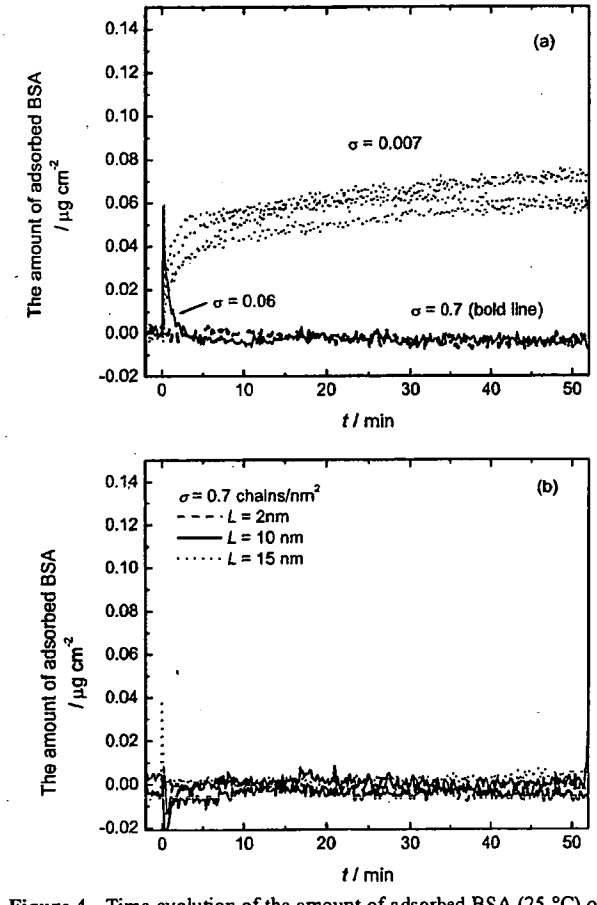

Figure 4. Time evolution of the amount of adsorbed BSA (25 °C) on (a) PHEMA brushes (σ = 0.007, 0.06, and 0.7 chains/nm^2) with L = 2 nm and (b) high-density PHEMA brushes (σ = 0.7 chains/nm^2) with L = 2, 10, and 15 nm. The BSA concentration was 1.0 g/L.

them. Figure 4 shows the results of the QCM measurement (25 °C) at an early stage of adsorption (<1 h), where the concentration of BSA in solution was .1 g/L. The adsorbed amount of BSA given in the ordinate axis was calculated from the frequency change according to eq 1. A sharp peak appearing, in some cases, immediately after the injection of BSA is due to the slight change in pressure and/or temperature on injection. The amount of BSA adsorbed onto the BHE-immobilized surface was 0.28 μg/cm^2 at 1 h (the data not shown), which is close to the value (0.25 μg/cm^2) reported for the side-on monolayer adsorption of BSA.[40] To confirm reproducibility of the measurement, we conducted at least five runs for each sample (an example is given for the low-density brush in Figure 4a, suggesting an experimental error of ±10%). BSA was readily (within 10 min) adsorbed on the low-density brush as well as the BHE surface and not desorbed by washing with PBS, indicating an irreversible adsorption. The amount of BSA adsorbed on the low-density brush at 1 h was ca. 0.07 μg/cm^2 (see Figure 4a), which is smaller than that for the BHE surface but still significant. On the other hand, there was no detectable adsorption on the middle- and high-density brushes (Figure 4a) with L = 2 nm. Figure 4b also shows that the high-density brushes with different thicknesses (L = 2, 10, and 15 nm) were all free from adsorption. These data clearly demonstrate that, by increasing the graft density, the adsorption of BSA can be suppressed. BSA has an ellipsoidal shape with an approximate dimension of 3 × 8 × 9 nm^3,[40–43] while the average distance d ($= \sigma^{-1/2}$) between the nearest-neighbor graft points is approximately 12, 4, and 1 nm for σ = 0.007, 0.06, and 0.7 chains/nm^2, respectively (Table 1). This reasonably suggests that BSA is difficult to diffuse into the swollen layer of the middle- and high-density brushes, on which no adsorption of BSA was, in fact, observed. The longer-term stability of protein repellency on the high-density brushes was studied by fluorescence microscopy, for the QCM experiment was difficult due to a baseline drift: no adsorption of FITC-BSA was detected on them even after 2 days.

Table 2. Absolute and Pullulan-Calibrated Molecular Weights, Crystallographic Dimensions, and $2R_g$ for Studied Proteins

protein	mol wt M	pullulan-calibrated M	crystallographic dimensions/nm	$2R_g$[a]/ nm
Aprotinin	6 500	1 500		2
Myoglobin	17 000	5 900	3 × 4 × 4	4
BSA	67 000	22 800	3 × 8 × 9	10
IgG	146 000	35 000		13

[a] Calculated (see text).

Adsorption of Proteins with Different Sizes. QCM experiments were conducted with the brush samples for a series of proteins with different sizes: Aprotinin (molecular weight = 6500), Myoglobin (17 000), BSA (67 000), and IgG (146 000). The characteristics of the four proteins are listed in Table 2. As the size of protein, crystallographic data are available for Myoglobin and BSA but not for the other two. The apparent molecular weights of these four proteins estimated by pullulan-calibrated GPC were 1500, 5900, 23 000, and 35 000 for Aprotinin, Myoglobin, BSA, and IgG, respectively, from which their radii of gyration (R_g) were estimated to be 1, 2, 5, and 6.5 nm, respectively, by using the known relation[44,45] between the R_g and molecular weight of pullulan. As shown in Table 2, the values of $2R_g$ may be good indices for the protein size (compare these values with the crystallographically determined dimensions of Myoglobin and BSA).

Figure 5 shows the amount of adsorbed protein after 1 h of soaking. The low-density brush adsorbed all the proteins, the middle-density one adsorbed only Aprotinin and Myoglobin, and the high-density one adsorbed none. These data show a clear dependence of adsorption on protein size and brush density: very crudely, we can state that no significant adsorption of protein takes place on a PHEMA brush when the brush d is smaller than the protein $2R_g$.

All these results confirm the size-exclusion effect of concentrated brushes. This effect would reduce the primary and tertiary adsorptions but not necessarily the secondary adsorption.

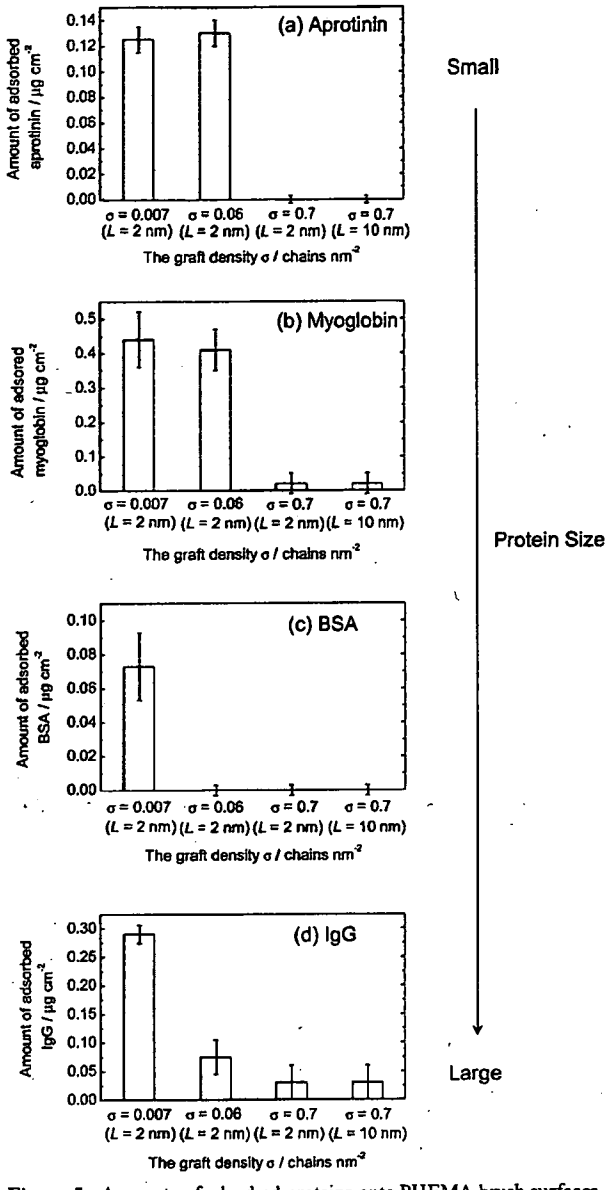

Figure 5. Amounts of adsorbed proteins onto PHEMA brush surfaces, soaked for 1 h (25 °C): (a) Aprotinin, (b) Myoglobin, (c) BSA, and (d) IgG. The protein concentration was 1.0 g/L in all cases.

The secondary adsorption can be induced by two possible interactions: one is the van der Waals and/or Coulombic interaction between the protein and the substrate, which should depend on the thickness of the brush layer.[15] The other is the interaction between the protein and the brush itself (at its outermost surface). The latter possibly depends on e.g. the water content of the brush layer,[46] the mobility of the brush chain,[47] and the structure of water near the brush surface.[31,32] Even though these details remain to be explored, the fact that no significant adsorption of any protein was detected on the high-density PHEMA brush indicates that the secondary adsorption is unimportant for this brush and these proteins. Figure 5 may indicate a nonnegligible adsorption of IgG on the high-density brush, but this may be ascribed to the insufficient number of trials, since another type of independent test (not shown here), which consisted of cycles of protein injection and rinsing, gave no indication of adsorption of this and other proteins on the high-density brush. To be stressed is the above-noted fact that the high-density brushes of different thickness repelled a protein (BSA) equally effectively. This means, on one hand, that no thick brush is needed for this purpose and, on the other hand, that a thick brush has a size-exclusion effect from its bottom to the outer surfaces through out. This is the very feature expected for a concentrated brush.

Finally, a comment is due regarding the block copolymer of PHEMA-PS type. Even though PHEMA cast films themselves have rather poor biocompatibility, as we have observed for the protein repellency, PHEMA-PS block copolymers are known to show improved biocompatibility.[48,49] At first, this improved biocompatibility was considered to have something to do with a microdomain surface structure caused by the phase separation of the PHEMA and PS segments. However, the ground for this interpretation seemed to have been lost, when the later structural studies on the cast films of these block copolymers revealed that the outermost surface of the films in water was preferentially covered with the laterally phase-separated PHEMA layer.[50–52] On the basis of our results, we would suggest the formulation of a concentrated brushlike structure of the PHEMA layer, in which the PHEMA chains are extruding out into the water phase from the hydrophobic (unswollen) PS layer, thereby repelling proteins or other large molecules by a size-exclusion effect.

Conclusions

The cast films and low-density brush ($\sigma = 0.007$ chains/nm^2) of PHEMA showed poor resistance against protein adsorption, which was reasonably ascribed to the tertiary adsorption, i.e., the adsorption induced by the interaction within the bulk of the PHEMA layer. On the other hand, the high-density brush ($\sigma = 0.7$ chains/nm^2) showed excellent resistance even for a protein as small as Aprotinin, independently of the brush thickness ($L = 2-15$ nm). The middle-density brush showed an intermediate behavior, adsorbing smaller proteins but effectively repelling larger proteins. There was a good correlation between the protein size and the threshold graft density beyond which the protein does not adsorb. (The secondary adsorption, occurring on the outermost surface of the PHEMA brushes, was inherently weak for the studied proteins.) These results confirmed the idea of size-exclusion effect of concentrated brushes. In general, it is suggested that the surface adsorption of large molecules like proteins can be greatly suppressed by densely grafting a polymer, i.e., controlling the *physical structure* of the polymer layer. With other unique properties of concentrated polymer brushes along with a range of possibility to design chain architecture by LRP, PHEMA concentrated brushes will find a wide variety of applications as a novel biointerface, such as biochips, biosensors, bioseparators, and medical body implants.

Acknowledgment. We thank Japan Analytical Industry (Tokyo) for the fractionation of PHEMA by preparative GPC. This work was supported by Grant-in-Aids for Scientific Research, the Ministry of Education, Culture, Sports, Science and Technology, Japan (Grant-in-Aids 17002007 and 17205022).

References and Notes

(1) Ejaz, M.; Yamamoto, S.; Ohno, K.; Tsujii, Y.; Fukuda, T. *Macromolecules* **1998**, *31*, 5934.
(2) Huang, X.; Wirth, M. J. *Macromolecules* **1999**, *32*, 1694.
(3) Matyjaszewski, K.; Miller, P. J.; Shukla, N.; Immaraporn, B.; Gelman, A.; Luokala, B. B.; Siclovan, T. M.; Kickelbick, G.; Vallant, T.; Hoffmann, H.; Pakula, T. *Macromolecules* **1999**, *32*, 8716.
(4) Husseman, M.; Malmstrom, E. E.; McNamara, M.; Mate, M.; Mecerreyes, D.; Benoit, D. G.; Hedrick, J. L.; Mansky, P.; Huang, E.; Russell, T. P.; Hawker, C. J. *Macromolecules* **1999**, *32*, 1424.
(5) Kim, J.-B.; Bruening, M. L.; Baker, G. L. *J. Am. Chem. Soc.* **2000**, *122*, 7616.
(6) Zhao, B.; Brittain, W. J. *Prog. Polym. Sci.* **2000**, *25*, 677.

(7) Pyun, J.; Kowalewski, Y.; Matyjaszewski, K. *Macromol. Rapid Commun.* **2003**, *24*, 1043.
(8) Edmonsdon, S.; Osborne, V. L.; Huck, W. T. S. *Chem. Soc. Rev.* **2004**, *33*, 14.
(9) Tsujii, Y.; Ohno, K.; Yamamoto, S.; Goto, A.; Fukuda, T. *Adv. Polym. Sci.*, in press.
(10) (a) Yamamoto, S.; Ejaz, M.; Tsujii, Y.; Matsumoto, M.; Fukuda, T. *Macromolecules* **2000**, *33*, 5602. (b) Yamamoto, S.; Ejaz, M.; Tsujii, Y.; Fukuda, T. *Macromolecules* **2000**, *33*, 5608.
(11) Yamamoto, S.; Tsujii, Y.; Fukuda, T. *Macromolecules* **2002**, *35*, 6077.
(12) Urayama, K.; Yamamoto, S.; Tsujii, Y.; Fukuda, T.; Neher, D. *Macromolecules* **2000**, *35*, 9459.
(13) Yamamoto, S.; Tsujii, Y.; Fukuda, T.; Torikai, N.; Takeda, M. *KENS Rep.* **2001–2002**, *14*, 204.
(14) He, H.; Tsujii, Y.; Fukuda, T.; Nakanishi, K.; Ishizuka, N.; Minakuchi, H. *Polym. Prepr., Jpn. (Soc. Polym. Sci., Jpn.)* **2003**, *52*, 2961.
(15) Currie, E. P. K.; Norde, W.; Cohen Stuart, M. A. *Adv. Colloid Interface Sci.* **2003**, *100–102*, 205.
(16) (a) Jeon, S. I.; Lee, J. H.; Andrade, J. D.; Degennes, P. G. *J. Colloid Interface Sci.* **1991**, *142*, 149. (b) Jeon, S. I.; Andrade, J. D. *J. Colloid Interface Sci.* **1991**, *142*, 159.
(17) Halperin, A. *Langmuir* **1999**, *15*, 2525.
(18) Unsworth, L. D.; Sheardown, H.; Brash, J. L. *Langmuir* **2005**, *21*, 1036.
(19) Norde, W.; Gage, D. *Langmuir* **2004**, *20*, 4162.
(20) Kenausis, G. L.; Voros, J.; Elbert, D. L.; Huang, N.; Hofer, R.; Ruiz-Taylor, L.; Textor, M.; Hubbel, J. A.; Spencer, N. D. *J. Phys. Chem. B* **2000**, *104*, 3298.
(21) Efremove, N. V.; Boundurant, B.; O'Brien, D. F.; Leckband, D. E. *Biochemistry* **2000**, *39*, 3441.
(22) Xiano, D.; Zhang, H.; Wirth, M. *Langmuir* **2002**, *18*, 9971.
(23) Lee, S. B.; Koepsel, R. R.; Morley, S. W.; Matyjaszewski, K.; Sun, Y.; Russell, A. J. *Biomacromolecules* **2004**, *5*, 877.
(24) Ma, H.; Hyun, J.; Stiller, P.; Chikoti, *A. Adv. Mater.* **2004**, *16*, 338.
(25) Feng, W.; Brash, J. L.; Zhu, S. *J. Polym. Sci., Part A: Polym. Chem.* **2004**, *42*, 2931.
(26) Iwata, R.; Suk-In, P.; Hoven, V. P.; Takahara, A.; Akiyoshi, K.; Iwasaki, Y. *Biomacromolecules* **2004**, *5*, 2308.
(27) Feng, W.; Zhu, S.; Ishihara, K.; Brash, J. L. *Langumuir*, in-press.
(28) Montheard, J. P.; Chatzopoulos, M.; Chappard, D. *J. Macromol. Sci., Rev. Macromol. Chem. Phys.* **1992**, *C32*, 1.
(29) (a) Ishihara, K.; Aragaki, R.; Ueda, T.; Watanabe, A.; Nakabayashi, N. *J. Biomed. Mater. Res.* **1990**, *24*, 1069. (b) Ishihara, K.; Ziats, N. P.; Tierney, B. P.; Nakabayashi, N.; Anderson, J. M. *J. Biomed. Mater. Res.* **1991**, *25*, 1397.
(30) Sawada, S.; Sakaki, S.; Iwasaki, Y.; Nakabayashi, N.; Ishihara, K. *J. Biomed. Mater. Res.* **2003**, *3*, 411.
(31) Tanaka, M.; Motomura, T.; Kawada, M.; Anzai, T.; Kasori, Y.; Shiroya, T.; Shimura, K.; Onishi, M.; Mochizuki, A. *Biomaterials* **2000**, *21*, 1471.
(32) Tanaka, M.; Mochizuki, A.; Motomura, T.; Shimura, K.; Onishi, M.; Okahata, Y. *Colloids Surf., A* **2001**, *193*, 145.
(33) Beers, L. K.; Boo, S.; Gaynor, S. G.; Matyjaszewski, K. *Macromolecules* **1999**, *32*, 5772.
(34) Ohno, K.; Morinaga, T.; Koh, K.; Tsujii, Y.; Fukuda, T. *Macromolecules* **2005**, *38*, 2137.
(35) Robinson, K. L.; Khan, M. A.; de Paz Banez, M. V.; Wang, X. S.; Armes, S. P. *Macromolecules* **2001**, *34*, 3155.
(36) Sauerbrey, G. *Z. Phys.* **1959**, *155*, 206.
(37) Jones, D. M.; Huck, W. T. S. *Adv. Mater.* **2001**, *13*, 1256.
(38) Zhou, F.; Liu, W.; Hao, J.; Chen, M.; Liu, W.; Sun, D. C. *Chem. Lett.* **2004**, *33*, 602.
(39) Huang, W.; Kim, J.-B.; Bruening, M. L.; Baker, G. L. *Macromolecules* **2002**, *35*, 1175.
(40) Baszkin, A.; Lyman, D. J. *J. Biomed. Mater. Res.* **1980**, *14*, 393.
(41) Suttiprasit, P.; Krisdhasima, V.; Mcguire, J. *J. Colloid Interface Sci.* **1992**, *154*, 316.
(42) Carter, D. C.; He, X.-M. *Science* **1990**, *249*, 302.
(43) Hook, F.; Rodahl, M.; Brzezinski, P.; Kasemo, B. *Langmuir* **1998**, *14*, 729.
(44) Asolphi, U.; Kulicke, W.-M. *Polymer* **1997**, *38*, 1513.
(45) Liy, J. H.-Y.; Brant, D. A.; Kitamura, S.; Kajiwara, K.; Mimura, M. *Macromolecules* **1999**, *32*, 8611.
(46) Tsuruta, T. *Adv. Polym. Sci.* **1996**, *126*, 1.
(47) (a) Fujimoto, K.; Inoue, H.; Ikada, Y. *J. Biomed. Mater. Res.* **1993**, *27*, 1559. (b) Fujimoto, K.; Tadokoro, H.; Ueda, Y.; Ikada, Y. *Biomaterials* **1993**, *14*, 442.
(48) Nojiri, C.; Nakahama, S.; Senshu, K.; Okano, T.; Kawagoishi, N.; Kido, T.; Sakai, K.; Koyanagi, H.; Akutsu, T. *ASAIO J.* **1993**, *39*, 322.
(49) Nojiri, C.; Senshu, K.; Okano, T. *Artif. Organs* **1995**, *19*, 32.
(50) Senshu, K.; Yamashita, S.; Ito, M.; Hirao, A.; Nakahama, S. *Langmuir* **1995**, *11*, 2293.
(51) Senshu, K.; Yamashita, S.; Mori, H.; Ito, M.; Hirao, A.; Nakahama, S. *Langmuir* **1999**, *15*, 1754.
(52) Senshu, K.; Kobayashi, M.; Ikawa, N.; Yamashita, S.; Hirao, A.; Nakahama, S. *Langmuir* **1999**, *15*, 1763.

MA0520242

Available online at www.sciencedirect.com
ScienceDirect
Biomaterials 28 (2007) 1–8
Biomaterials
www.elsevier.com/locate/biomaterials

Preparation and characterization of cross-linked collagen–phospholipid polymer hybrid gels

Kwangwoo Nam, Tsuyoshi Kimura, Akio Kishida*

Division of Biofunctional Molecules, Institute of Biomaterials and Bioengineering, Tokyo Medical and Dental University, 2-3-10 Kanda-Surugadai, Chiyoda-ku, Tokyo 101-0062, Japan

Received 5 June 2006; accepted 1 August 2006
Available online 7 September 2006

Abstract

2-methacryloyloxyethyl phosphorylcholine (MPC)-immobilized collagen gel was developed. Using 1-ethyl-3-(3-dimethyl aminopropyl)-1-carbodiimide hydrochloride (EDC) and *N*-hydroxysuccinimide (NHS), we cross-linked a collagen film in 2-morpholinoethane sulfonic acid (MES) buffer (EN gel). EN gel was prepared under both pH 4.5 and pH 9.0 in order to observe changes in cross-linking ability. To cross-link MPC to collagen gel, poly(MPC-*co*-methacrylic acid) (PMA) having a carboxyl group side chain was chosen. E/N gel was added to the MES buffer having pre-NHS activated PMA to make MPC-immobilized collagen gel (MiC gel). MiC gel was prepared under both acidic and alkaline conditions to observe the changes in the cross-linking ability of PMA. X-ray photoelectron spectroscopy showed that the PMA was cross-linked with collagen under both acidic and alkaline conditions. Differential scanning calorimetry (DSC) results showed that the shrinkage temperature increased for the MiC gels and that the increase would be greater for the MiC gel prepared under alkaline conditions. The data showed that swelling would be less when the MiC gel was prepared under alkaline conditions. The biodegradation caused by collagenase was suppressed for the MiC gel prepared under alkaline conditions due to stable inter- and intrahelical networks.

Keywords: Collagen; Phospholipid; Cross-linking; Surface modification

1. Introduction

Collagen is an extracellular-matrix protein that plays an important role in the formation of tissues and organs and is involved in various functional expressions of cells [1]. Collagen is non-toxic, non-antigenic, favors cell adhesion, proliferation, and differentiation to mimic the natural cell environment. However, favoring cell adhesion can be both advantageous and disadvantageous, for its strong affinity to cells and blood is uncontrollable, which may soon lead to blood coagulation and mineralization when applied for use as artificial blood vessels. Furthermore, the collagen that is prepared in a matrix form such as a gel for tissue reconstruction is mechanically insufficient [2]. Without modification, the collagen gel cannot be applied for bioprosthesis [3].

To overcome the disadvantages of collagen while maintaining its biological performance, a prosthesis-tissue complex, or bioartificial polymeric material, was developed by blending or mixing biomolecules and synthetic materials. The chief purpose for developing such a bioartificial polymer material is to overcome the poor biological performance of synthetic polymers and to enhance the mechanical characteristics of biomolecules [4].

To control cell adhesiveness and to increase mechanical strength simultaneously, collagen must be modified by cross-linking or mixing with synthetic polymers. Polymers such as poly(vinyl alcohol), poly(acrylic acid), poly(vinyl pyrrolidone), and polyethylene are used as bioartificial polymer materials because of their favorable chemical reactivity with collagen, absence of toxicity, and good mechanical performance [4–8].

However, it is very important to consider biological response in the adoption of a cross-linker or synthetic polymer because of the possibilities of severe problems

*Corresponding author. Tel./fax: +81 03 5280 8028.
E-mail address: kishida.fm@tmd.ac.jp (A. Kishida).

0142-9612/$ - see front matter © 2006 Elsevier Ltd. All rights reserved.
doi:10.1016/j.biomaterials.2006.08.002

such as toxicity, inflammatory response, or alteration of protein structure. Furthermore, some synthetic polymers that are known to be 'biocompatible' degrade in biological fluids, making the collagen structure unstable. Adoption of natural cross-linkers such as glutaraldehyde [9], genipin [10], or transglutaminase [11], and natural polymers like hyaluronic acid [12], heparin [13], or chondroitin-6-sulfate [14,15] is used as direct cross-linker or immobilizer to overcome the problems presented by the use of synthetic polymers, but cannot fully solve the problems.

To overcome these problems, we developed a biosynthetic hybrid material by cross-linking collagen with a 2-methacryloyloxyethyl phosphorylcholine (MPC) based copolymer using *N*-(3-dimethylaminopropyl)-*N'*-ethylcarbodiimide (EDC) and *N*-hydroxysuccinimide (NHS) as cross-linkers by activating the MPC polymer with EDC and NHS to cross-link the microfibrils and polymer chain using amide bond [3,16–18].

MPC is a blood compatible product developed in the early 1990s [19]. Design of the MPC polymer took into account the surface structure of the biomembrane. Recently, phospholipid-accumulated surfaces have been prepared by various methods, and it has been reported that the phosphorylcholine group plays an important role showing excellent blood compatibility and anti-protein adsorptivity [20–23]. The MPC units can then be introduced to conventional polymers by various methods of modification. They effectively reduce protein adsorption and denaturation and inhibit cell adhesion even when the polymer is exposed to whole blood in the absence of any anticoagulants [24]. By adopting the MPC polymer with the collagen gel, it is possible to expect a biocompatible collagen–polymer hybrid gel that is stable, has its molecular weight controlled, has no cross-linker leaking, and is mechanically tough.

In the present study, cross-linking ability between poly(MPC-*co*-methacrylic acid) (PMA) and collagen using EDC and NHS was investigated by altering several parameters, and the physical properties of PMA-immobilized matrices were characterized. In this article, the terms interchain cross-linking and immobilization are used synonymously.

2. Experimental method

2.1. Preparation of collagen–phospholipid polymer hybrid gel

2.1.1. Synthesis of PMA

PMA was synthesized by a method that has already been published [19]. In short, desired amount of MPC and MA was dissolved in ethanol in an ampoule. Then 2,2'-azoisobutyronitrile (AIBN) was added to the ethanol solution. The argon gas was bubbled into the ethanol solution to eliminate the oxygen. The ampoule was sealed and heated to 60 °C for 16 h. The solution was precipitated into diethyl ether, freeze-dried, and kept in vacuum until use. The mole ratio of PMA was controlled to MPC:MA = 3:7, and the number average molecular weight $\overline{M}_n$ of the PMA was approximately 300,000. The chemical structure of PMA is shown in Fig. 1.

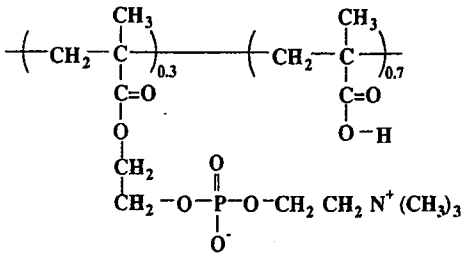

Fig. 1. Chemical structure of PMA.

Table 1
Terminology of collagen gels used in this study

Terminology	Composition
Uc-gel	Uncross-linked collagen gel (immersed in alkaline pH conditions)
EN-1	EDC/NHS-cross-linked collagen gel under acidic pH conditions
EN-2	EDC/NHS-cross-linked collagen gel under alkaline pH conditions
MiC-11 gel	PMA immobilized to EN-1 gel under acid pH conditions
MiC-12 gel	PMA immobilized to EN-1 gel under alkaline pH conditions
MiC-21 gel	PMA immobilized to EN-2 gel under acid pH conditions
MiC-22 gel	PMA immobilized to EN-2 gel under alkaline pH conditions

2.1.2. Preparation of EDC and NHS cross-linked collagen gel (EN gel)

Cross-linked collagen gel was prepared by using 0.5 wt% collagen type I solution (pH 3, KOKEN, Tokyo, Japan). Conventional film fabrication method was used for the film fabrication. The collagen solution was dropped onto the polyethylene film and dried in room temperature. The collagen film (thickness = 36 ± 2 μm) was immersed into a 0.05 M 2-morpholinoethane sulfonic acid (MES) buffer (pH 4.5) (Sigma, St. Louis, USA) containing 1-ethyl-3-(3-dimethyl aminopropyl)-1-carbodiimide hydrochloride (EDC) (Kanto Chemicals, Tokyo, Japan) and NHS (Kanto Chemicals, Tokyo, Japan). Each chemical was added at the mole ratio of EDC:NHS:collagen-carboxylic acid groups = 5:5:1 [11,13]. The cross-linking procedure was allowed to continue for 4 h at 4 °C to produce a cross-linked gel (EN-1 gel). After 4 h, the reaction was stopped by removing the gel from the solution. The gel was then washed with 4 M of Na_2HPO_4 aqueous solution for 2 h to hydrolyze any remaining *O*-acylisourea groups and then with distilled water for 3 days to remove any salts from the gel. Same preparation process was repeated under alkaline conditions (pH 9.0; adjusted with NaOH) to prepare an EN-2 gel.

2.1.3. Preparation of MPC-immobilized collagen gel (MiC gel)

Preparation of the MiC gel was done by using the EN-1 and EN-2 gels. PMA was added with EDC and NHS to the MES buffer (pH 4.5 and pH 9.0) and was pre-activated for 10 min before immersion of the EN-1 or EN-2 gel. The immobilization of PMA to the collagen was allowed to continue for 4 h at 4 °C. The gel was then washed with 4 M of Na_2HPO_4 aqueous solution for 2 h and then with distilled water for 1 day to remove any salts from the gel to prepare a salt-free MiC gel: MiC-11 gel (PMA immobilized under acidic conditions using the EN-1 gel), MiC-12 gel (PMA immobilized under alkaline conditions using the EN-1 gel), MiC-21 gel (PMA immobilized under acidic conditions using the EN-2 gel), and MiC-22 gel (PMA immobilized under alkaline conditions using the EN-2 gel). The terminology of the samples is listed in Table 1. PMA cross-linking with the collagen is shown in Fig. 2. Collagen film was immersed

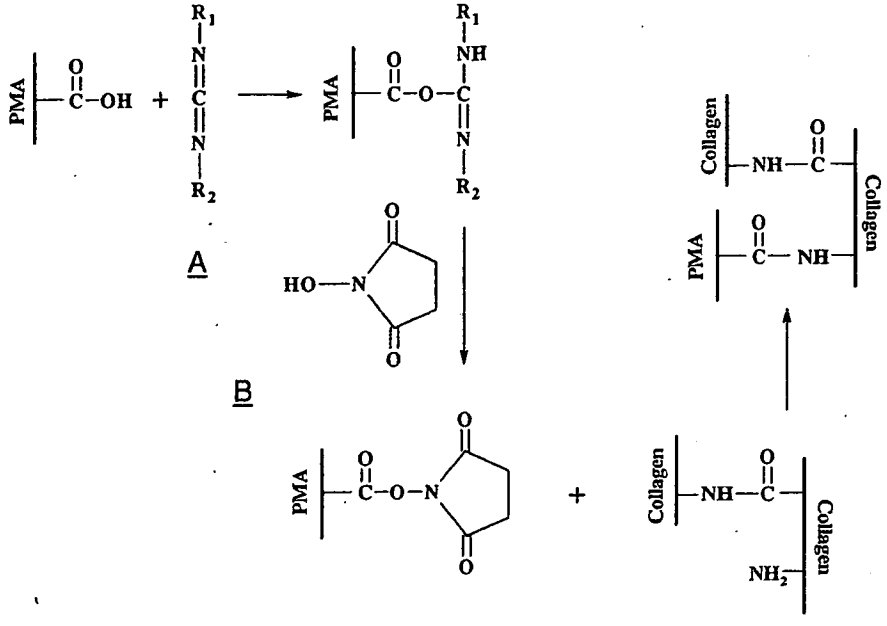

A: 1-ethyl-3-(3-dimethylaminopropyl)-1-ethylcarbodiimide hydrochloride (EDC)
B: *N*-hydroxysuccinimide (NHS)

Fig. 2. Schematic picture of immobilization of MPC polymer with collagen.

into the MES buffer pH 9.0 for 1 day to obtain a non cross-linked collagen gel (Uc-gel) and was used as a reference.

2.2. Characterization

2.2.1. Surface analysis

Surface analysis was executed using X-ray photoelectron spectroscopy (XPS, AXIS-HSi, Shimadzu/KRATOS, Kyoto, Japan) and scanning electron microscopy (SEM, SM-200, Topcon, Tokyo, Japan). The samples, which had been cut into small pieces, were lyophilized overnight. The chemical composition of the surfaces of the gel was determined by the take-off angle of the photoelectrons fixed at 90°. The morphologies of the gels were observed with SEM after gold coating with an ion coater (IB-3, Eiko Co., Ibaraki, Japan). The razor blade-cut surfaces of the respective gels were observed.

2.2.2. Shrinkage temperature

The shrinkage temperatures of the gels were determined using differential scanning calorimetry (DSC, DSC6000, Seiko, Chiba, Japan) in the range 0–150 °C at a scanning rate 5 °C/min. The samples were incubated with small amounts of phosphate buffer solution for 1 h at room temperature before being measured [9]. Instead of an empty container, a container of PBS was used for reference.

2.2.3. Mechanical properties

The stress–strain curves of the respective collagen gels were determined by uniaxial measurements using a universal testing machine (Orientec STA-1150, Tokyo, Japan). The sizes of the samples used for measurement were 4 cm × 1 cm. Each sample was strained at the rate of 10 mm/min. The obtained data were fitted to the stress–strain curves of the samples and the elongational modulus at 1% and 8% was calculated.

2.2.4. Swelling test

A swelling test of each sample was executed by cutting the lyophilized gels into small pieces and putting them into pH-controlled aqueous solutions at 37 °C. The pH of the aqueous solution was controlled to 2.1 or 7.4. The gels were gently shaken for 24 h and then removed for weighing. The swelling ratio was calculated in order to define the exact amount of swelling caused by water absorption. The equation used for the swelling ratio was

$$\text{Swelling ratio, } S(\%) = \frac{W_h - W_d}{W_d} \times 100$$

where W_h is hydrated weight and W_d is dried weight of the gel.

2.2.5. Enzymatic degradation test

Degradation tests of the gel samples were executed using collagenase from Clostridiopeptidase histoluticum (EC 3.4.24.3, *Sigma*, St. Louis, USA) with collagenase activity of 300 units/mg. In this experiment, 30±2 mg of collagen gels were immersed into 2 mL of 0.1 M Tris-HCl buffer (pH 7.4) with 5×10^{-3} M of calcium chloride (Kanto Chemical, Tokyo, Japan) and 8×10^{-4} M of sodium azide (Kanto Chemicals, Tokyo, Japan) and was shaken for 1 h at 37 °C. Then, 2 mL of collagenase Tris-HCl buffer solution with a concentration of 1.32 mg/mL was added to the solution containing the gel to determine the total concentration of collagenase at 100 units/mL. The container was returned to the shaking water bath. The remaining weights of the samples were measured for 72 h.

2.2.6. Statistical analysis

All experiments were repeated at least three times and the values are expressed as mean ±standard deviation. In several figures, the error bars are not visible because they are included in the plot. Statistical analyses were performed using student's *t*-test. The level of significance was set as $P<0.05$.

3. Results and discussion

3.1. Basic characteristics of collagen gels

The reaction between EDC and the carboxyl groups are shown elsewhere; the mechanism is well known [25,26]. According to Nakajima and Ikada [26], proton and ionized carboxyl groups are required for the reaction with EDC. The excess amount of EDC against the carboxyl groups should be used up, and no reaction occurred when the molar ratio of EDC to the carboxyl groups was below 0.5. Using EDC for cross-linking might cause hydrolysis, which makes the carboxyl groups return to the original carboxyl groups.

The use of NHS is to prohibit the hydrolysis of the carboxyl groups. NHS would lead to formation of NHS-ester, which prevents the side reaction of the *O*-acylisourea groups [25,26]. This is because the reactive species relative to the neucleophilic attack of the free amine group of collagen are the NHS-activated carboxyl groups rather than the *O*-acylisourea groups.

Fig. 3 shows the XPS result of Uc-gel, EN-2 gel, MiC-21 gel, and MiC-12. All gels showed XPS signals attributed to carbon in CH_3– or –CH_2–, –COC–, C(=O)–, and nitrogen in –CONH– was observed at 285, 286.6, 288.5, and 400.8 eV, respectively. The phosphorus peak and one nitrogen peak in $-N^+(CH_3)_3$ were observed at 134 and 403.2 eV, respectively, indicating that PMA was a properly cross-linked collagen [21,24].

SEM images of the outer surfaces and razor blade-cut surfaces (vertical cross-section) of the respective collagen gels are shown in Fig. 4. The razor blade-cut surfaces of the Uc-gel and the EN-1 and EN-2 gels are porous. For MiC, the non-porous layer is shown to be deposited on the porous layer. Non-porosity can be seen for the pure PMA film prepared using same method (image not shown). This implies that PMA covers the collagen gel instead of being blended, making it a heterogeneous phase. However, the outer surface of the gel is entirely one phase showing no defects, indicating that PMA is immobilized on the collagen surface and is distributed homogeneously. This is because the high molecular weight of the PMA causes the polymer to be located primarily on the surface of the collagen gel. When the PMA and collagen are premixed and gelled, the razor blade-cut surface shows that the porous and non-porous structures coexist (picture not shown). In the case of MiC-11 and MiC-12, the non-porous outer layer is very thin and the pore size is bigger, indicating that a sizeable amount of swelling had occurred.

3.2. Network structure of collagen gels

Shrinkage temperature T_s is considered as the rupture of the inter-chain bonds bringing the fusion of the oriented peptide chains [27], which is responsible for the shrinkage, and the cross-linking will result in the stabilization of the triple helix structure and an increase in the shrinkage temperature [28]. Table 2 lists T_s of the respective collagen gels. The result indicates that T_s would increase when the gels are cross-linked. Because PMA is immobilized, T_s of the gels would shift to a higher temperature, eventually reaching approximately 85 °C, which is about a 30 °C increase from that of uncross-linked collagen gel. The EN-1 gel and the MiC-11 and MiC-12 gels showed that T_s is lower than the EN-2 gel and the MiC-21 and MiC-22 gels. This implies that formation of inter- and intrahelical cross-links, which prevent the fusion of the peptide chains, is very important for stabilization of the network. The immobilization of PMA made the extra cross-link, that is, the bond between the PMA chain and collagen microfibril by the amide bond, eventually increasing T_s further. Comparing T_s of MiC-11 and MiC-12, we can see that the numeric value is almost the same. The same phenomenon can be seen for MiC-21 and MiC-22, implying that the immobilization of PMA would be affected by the pH of the MES buffer. Under pH 4.5, the carboxyl groups of PMA would be protonated, leading to the formation of COO–NHS, because the pK_a of PMA is known to be 2.7 [29].

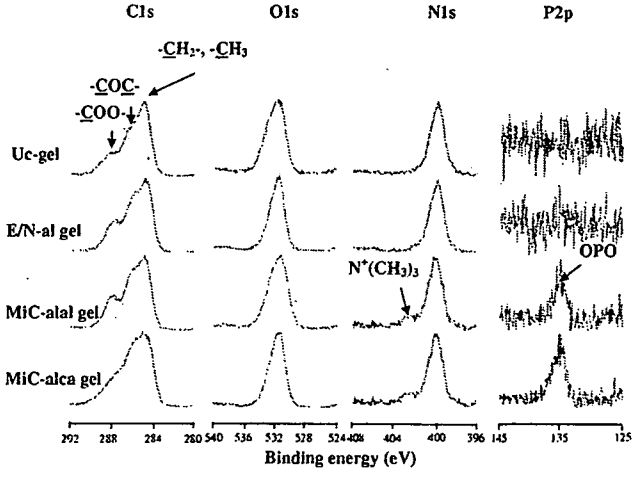

Fig. 3. XPS chart of Uc-gel, E/N-21 gel, MiC-22 gel, and MiC-21 gel. The takeoff angle of photoelectron was 90°.

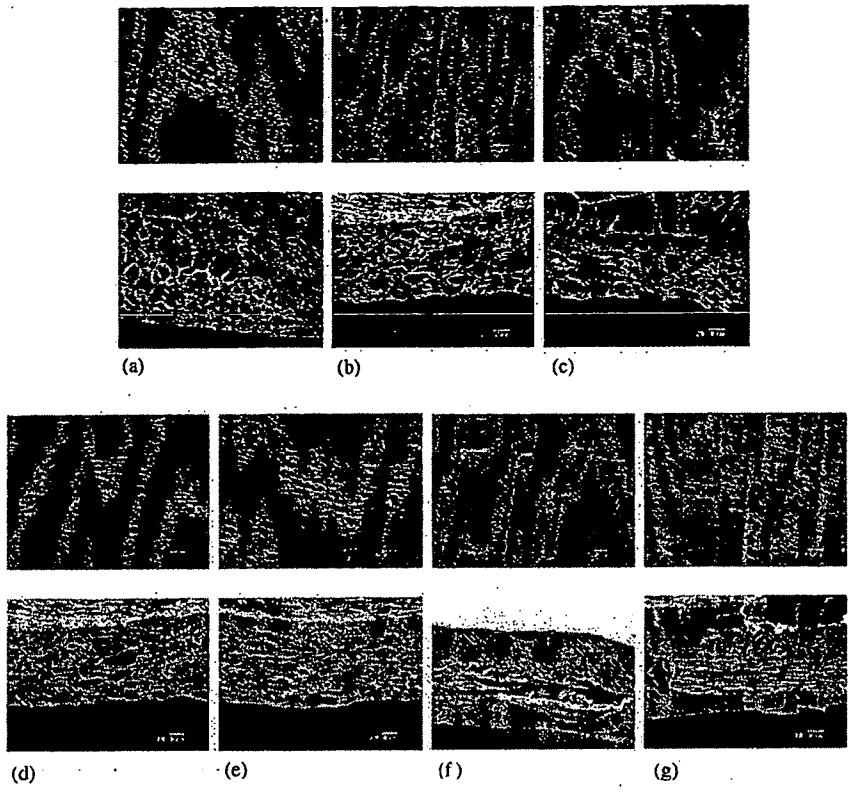

Fig. 4. Outer surface morphology (upper) and razor blade cut morphology (below) of respective gels: (a) Uc-gel, (b) E/N-1 gel, (c) E/N-2 gel, (d) MiC-11 gel, (e) MiC-12 gel, (f) MiC-22 gel, and (g) MiC-21 gel.

Table 2
Shrinkage temperatures of collagen and collagen gels

Sample	T_s (°C)
Uncross-linked	56.4±8.1
EN-1	67.4±0.9
EN-2	76.5±2.9
MiC-11	74.1±3.9
MiC-12	75.1±2.0
MiC-21	84.8±2.0
MiC-22	84.1±3.9

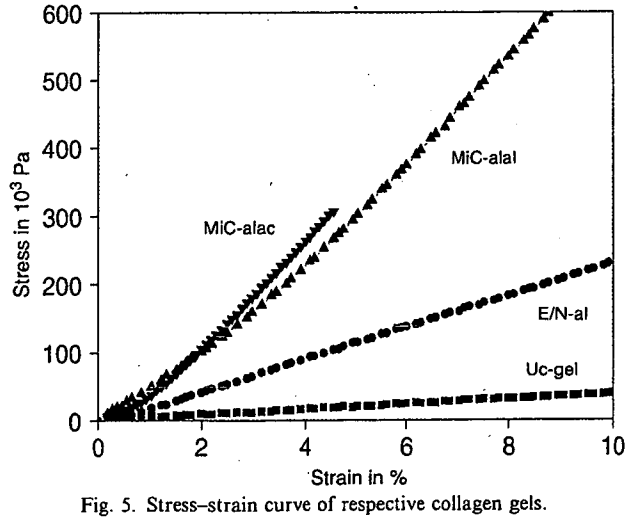

Fig. 5. Stress–strain curve of respective collagen gels.

Fig. 5 shows the strain–stress curve of the Uc-gel, EN-2 gel, MiC-22, and MiC-21 gels. It can be seen that all collagen gels are J-shaped. This shape indicates that, after the cross-linking and immobilization processes, the collagen maintains its soft tissue viscoelastic behavior, which is soft and tough [30]. Table 3 shows the results of the elongational strain modulus of the respective gels at 1% and 8% of strain. Cross-linking with EDC/NHS increased the elongational strain modulus approximately five times and immobilization of PMA increased the elongational strain modulus about 12.5 times that of the uncross-linked collagen gel. The cross-linking process and immobilization of PMA made the collagen gel much tougher. This strongly suggests that the PMA must be immobilized onto the surface of the collagen gel in order to maintain its biomolecular property and stronger mechanical property simultaneously. The EN-1 gel, MiC-21, and MiC-11 gels were too fragile to measure the strain modulus.

Fig. 6 shows the swelling of the respective gels under pH 2.4 and pH 7.4. For uncross-linked gels, the gel dissolved under pH 2.4, while it swelled approximately 1400% under pH 7.4. When collagen gels absorb water, the triple helix structure is known to turn into a random coil conformation because the collagen peptide chains increase the accessibility to hydration. In the neutral and alkaline

Table 3
Mechanical strength of the collagen gels

Sample	Strain modulus at 1% (MPa)	Strain modulus at 8% (MPa)
Uncross-linked	0.4±0.1	0.6±0.1
EN-2 gel	2.1±0.1	2.9±0.2
MiC-21	5.6±1.1	8.7±1.6
MiC-21	5.1±0.6	8.0±1.0

Mechanical strength of EN-1, MiC-11 and MiC-12 was not measured due to fringe nature of the samples.

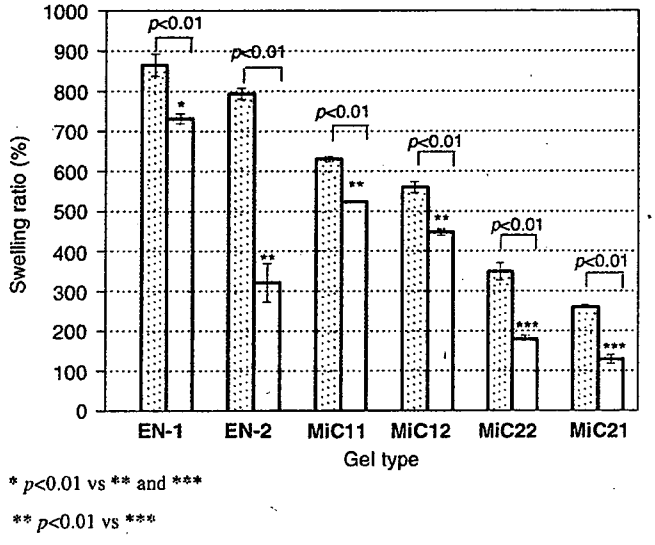

Fig. 6. Swelling ratio of respective collagen gels under pH 2.1 (hatched bar) and under pH 7.4 (empty bar) aqueous solutions. Each value represents the mean±SD ($n = 5$).

conditions, collagen film would be stabilized by forming an entanglement of fibrils formed by hydrophobic and electrostatic bonds [31–33]. Since the pK_a of collagen type I is known to be approximately 5.5 [34,35], a stable gel without any cross-linker can be formed under neutral and alkaline conditions.

The EN-1 and EN-2 gels showed a high swelling ratio under pH 2.1, but had different swelling ratios under neutral pH conditions. The EN-1 gels showed a swelling ratio of about 870% under pH 2.4 and 730% under pH 7.4, while the EN-2 gels showed 800% under pH 2.4 and 320% under pH 7.4. The swelling ratio was relatively higher for the EN-1 gel than the EN-2 gel because the network density was much higher for the EN-2 gel. The EN-2 gel, for which cross-linking was executed under alkaline conditions, is thought to possess a denser cross-linking network. As mentioned earlier, EDC and NHS are known to bring inter- and intrahelical cross-links, holding the α-helices together tightly. [36,37].

Immobilization of PMA on the collagen gels brought different swelling ratios according to the conditions of preparation. For the MiC-11 and MiC-12 gels, the swelling ratio was lower than that for the EN-1 gel, implying that a network between collagen and PMA is formed by the interchain cross-links. However, their swelling ratio under pH 2.4 was lower than that for the EN-2 gel, but was higher under pH 7.4. PMA could not penetrate into the collagen gel during the immobilization process, leaving much of the amine groups unreacted. In contrast, MiC-21 and MiC-22 showed that the swelling ratio under pH 2.4 and pH 7.4 would be lowest among all collagen gels. As mentioned earlier, the formation of a denser network brought a lower swelling ratio. The low swelling ratio of the MiC-11 and MiC-12 gels under pH 2.4 and pH 7.4 implies that the intra- and interhelical cross-links play important roles in the stabilization of the collagen gels.

3.3. Degradation of collagen gels by collagenase

Fig. 7 shows the degradation of collagen gels caused by the activation of collagenase in Tris-HCl buffer. The collagenase absorbed into the collagen gel would cleave the helical segment, hydrolyzing the collagen gels. Collagenase is known to be adsorbed onto the collagen fibers once it penetrates into the fiber [36–39]. Therefore, it is thought that the swelling ratio is related to this biodegradation process.

Our study shows that the collagen gel that is not cross-linked would degrade within 2 or 3 h. Cross-linking the collagen with EDC and NHS would strongly maintain the helical structure, extending the time of complete degradation from 6 to 24 h according to the cross-linking conditions. Low swelling collagen gels lead to slow degradation. For the MiC-22 and MiC-21 gels, almost 80% of the original collagen gel remained after 24 h. The E/N gels have only intra- and interhelical cross-links while the MiC gels possess interchain cross-links. For the E/N

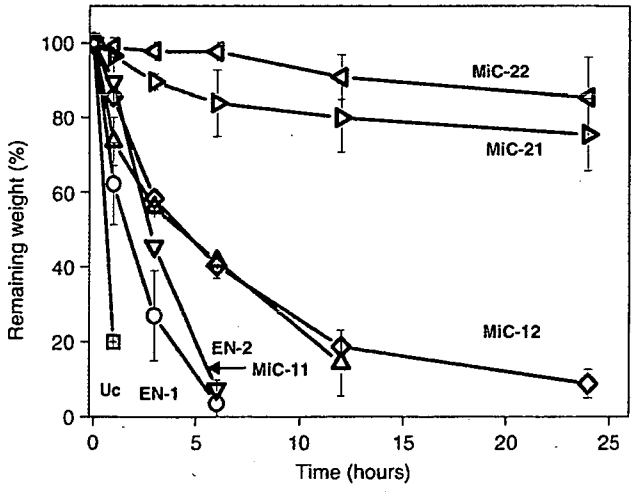

Fig. 7. Degradation of collagen gels by collagenase in Tris-HCl buffer (pH 7.4) at 37 °C. Each value represents the mean±SD ($n = 4$).

gels, the intra- and interhelical cross-links maintained the helical structure after cleavage by collagenase [39]. However, the absorption of water eventually made the E/N gels dissociate within 24 h, with slightly faster degradation for the EN-1 gel. In contrast, the MiC gels possess interchain cross-links that link the microfibrils and the PMA chains, making the degree of swelling much lower [38]. The cleavage by collagenase would be prevented by the PMA-collagen network, which links microfibrils together, shielding the helices.

4. Conclusion

We were able to successfully immobilize MPC to collagen and prepare a stable gel. By using collagen film prepared from 0.5 wt% collagen solution, MiC gels were prepared under MES buffer. EDC/NHS and PMA polymer could form a cross-link with the collagen film. The physical behaviors of the gels changed according to the preparation conditions such as the pH of the MES buffer. Inter- and intrahelical cross-links were formed by EDC/NHS. Higher cross-link efficiency can be obtained under an alkaline condition because the pK_a of collagen is approximately 5.5. A pre-NHS activated PMA polymer chain could be located on the collagen gel and cross-linked with the amine collagen group, forming an interchain cross-link. Since the pK_a of PMA carboxyl groups is 2.7, the immobilization of PMA was successful at any pH. The coexistence of intra- and interhelical cross-links and intermolecular cross-links make the network much denser, which leads to difficulty in either penetration or hydrolyzation by the collagenase. Mechanical and enzyme stability enable this gel to be applied as a biosynthetic hybrid biomaterial.

We will report on the biological properties of the collagen–phospholipid polymer hybrid gel in the near future.

Acknowledgment

This study was financially supported by a grant from the Research on Health Sciences Focusing on Drug Innovation (KH61060) of the Japan Health Sciences Foundation and Health and Labour Sciences Research Grants (HLSRG).

We would like to thank Professor Kazuhiko Ishihara of The University of Tokyo for his helpful advice on phospholipid polymer.

References

[1] Fujioka K, Maeda M, Hojo T, Sano A. Protein release from collagen matrices. Adv Drug Deliv Rev 1998;31:247–66.
[2] Kato YP, Silver FH. Formation of continuous collagen fibers: evaluation of biocompatibility and mechanical properties. Biomaterials 1990;11:169–75.
[3] Olde Damink LHH, Dijkstra PJ, van Luyn MJA, van Wachem PB, Nieuwenhuis P, Feijen J. Crosslinking of dermal sheep collagen using a water-soluble carbodiimide. Biomaterials 1996;17:765–73.
[4] Cascone MG, Barbani N, Cristalli C, Giusti P, Ciardelli G, Lazzeri L. Bioartificial polymer materials based on polysaccharides. J Biomater Sci Polym Edn 2001;12:267–81.
[5] Barbani N, Lazzeri L, Cristalli C, Cascone MG, Polacco G, Pizzirani G. Bioartificial materials based on blends of collagen and poly(acrylic acid). J Appl Polym Sci 1999;72:971–6.
[6] Cascone MG, Martinti S, Barbani N, Laus M. Effect of chitosan and dextran on the properties of poly(vinyl alcohol) hydrogels. J Mater Sci Mater Med 1999;10:431–5.
[7] Sionkowska A. Interaction of collagen and poly(vinyl pyrrolidone) in blends. Eur Polym J 2003;39:2135–40.
[8] Dascălu MC, Vasile C, Silvestre C, Pascu M. On the compatibility of low density polyethylene/hydrolyzed collagen blends. II: new compatibilizers. Eur Polym J 2005;41:1391–402.
[9] Olde Damink LHH, Dijkstra PJ, van Luyn MJA, van Wachem PB, Nieuwenhuis P, Feijen J. Glutaraldehyde as a crosslinking agent for collagen-based biomaterials. J Mater Sci Mater Med 1995;6:460–72.
[10] Sung HW, Chang WH, Ma CY, Lee MH. Crosslinking of biological tissue using genipin and/or carbodiimide. J Biomed Mater Res 2003;64A:427–38.
[11] Orban JM, Wilson LB, Kofroth JA, El-Kurdi MS, Maul TM, Vorp DA. Crosslinking of collagen gels by transglutaminase. J Biomed Mater Res 2004;68:756–62.
[12] Segura T, Chung PH, Shea LD. DNA delivery from hyaluronic acid–collagen hydrogels via a substrate-mediated approach. Biomaterials 2005;26:1575–84.
[13] Wissink MJB, Beernink R, Pieper JS, Poot AA, Engbers GHM, Beugeling T, et al. Immobilization of heparin to EDC/NHS-crosslinked collagen, characterization and in vitro evaluation. Biomaterials 2001;22:151–63.
[14] Perper JS, Hafmans T, Veerkamp JH, van Kuppevelt TH. Development of tailoir-made collagen-glycosaminoglycan matrices: EDC/NHS crosslinking, and ultrastructural aspects. Biomaterials 2000;21:581–93.
[15] Jaworski J, Klapperich CM. Fibroblast remodeling activity at two- and three-dimensional collagen–glycosaminoglycan interfaces. Biomaterials 2006;23:4212–20.
[16] van Luyn MJA, van Wachem PB, Olde Damink LHH, Dijkstra PJ, Feijen J. Relations between in vitro cytotoxicity and crosslinked dermal sheep collagens. J Biomed Mater Res 1992;26:1091–110.
[17] van Wachem PB, van Luyn MJA, Olde Damink LHH, Dijkstra PJ, Nieuwenhuis P. Biocompatibility and tissue regenerating capacity of crosslinked dermal sheep collagen. J Biomed Mater Res 1994;17:353–63.
[18] van Wachem PB, Zeeman R, Dijkstra PJ, Feijen J, Hendriks M, Cahalan PT, et al. Characterization and biocompatibility of epoxy-crosslinked dermal sheep collagens. J Biomed Mater Res 1999;47:270–7.
[19] Ishihara K, Ueda T, Nakabayashi N. Preparation of phospholipid polymers and their properties as polymer hydrogel membranes. Polym J 1990;22:355–60.
[20] Iwasaki Y, Mikami A, Kurita K, Yui N, Ishihara K, Nakabayashi N. Reduction of surface-induced platelet activation on phospholipid polymer. J Biomed Mater Res 1997;36:508–15.
[21] Ishihara K, Nomura H, Mihara T, Kurita K, Iwasaki Y, Nakabayashi N. Why do phospholipid polymers reduce protein adsorption? J Biomed Mater Res 1998;39:323–30.
[22] Kitano H, Imai M, Mori T, Gemmei-Ide M, Yokoyama Y, Ishihara K. Structure of water in the vicinity of phospholipid analogue copolymers as studied by vibrational spectroscopy. Langmuir 2003;19:10260–6.
[23] Ueda H, Watanabe J, Konno T, Takai M, Saito A, Ishihara K. Asymmetrically functional surface properties on biocompatible phospholipid polymer membrane for bioartificial kidney. J Biomed Mater Res A 2006;77:19–27.

[24] Watanabe J, Ishihara K. Phosphorylcholine and poly(D,L-lactic acid) containing copolymers as substrates for cell adhesion. Artif Organs 2003;27:242–8.
[25] Olde Damink LHH, Dijkstra PJ, van Luyn MJA, van Wachem PB, Nieuwenhuis P, Feijen J. In vitro degradation of dermal sheep collagen crosslinked using a water-soluble carbodiimide. Biomaterials 1996;17:679–84.
[26] Nakajima N, Ikada Y. Mechanism of amide formation by carbodiimide for bioconjugation in aqueous media. Bioconjugate Chem 1995;6:123–30.
[27] Flory PJ, Garrett RR. Phase transitions in collagen and gelatin systems. J Am Chem Soc 1958;80:4836–45.
[28] Khor E, Li HC, Wee A. Animal tissue-polypyrrole hybrid biomaterials: shrinkage temperature evaluation. Biomaterials 1996;17:1877–9.
[29] Nam K, Watanabe J, Ishihara K. Modeling of swelling and dissociation mechanism, and release behavior of spontaneously forming hydrogel composed of phospholipid polymers for oral delivery carrier. Int J Pharma 2004;275:259–69.
[30] Gentleman E, Lay AN, Dickerson DA, Nauman EA, Livesay GA, Dee KA. Mechanical characterization of collagen fibers and scaffolds for tissue engineering. Biomaterials 2003;24:3805–13.
[31] Ripamonti A, Roveri N, Briga D. Effects of pH and ionic strength on the structure of collagen fibrils. Biopolymers 1980;19:965–75.
[32] Wallace D. The relative contribution of electrostatic interactions to stabilization of collagen fibrils. Biopolymers 1990;29:1015–26.
[33] Rosenblatt J, Devereux B, Wallace D. Dynamic rheological studies of hydrophobic interactions in injectable collagen biomaterials. J Appl Polym Sci 1993;50:953–63.
[34] Luescher M, Ruegg M, Schindler P. Effect of hydration upon the thermal stability of tropocollagen and its dependence on the presence of neutral salts. Biopolymers 1974;13: 2489–503.
[35] Zhang J, Senger B, Vautier D, Picart C, Schaaf P, Voegel J-C, et al. Natural polyeletrolyte films based on layer-by-layer deposition of collagen and hyaluronic acid. Biomaterials 2005;26: 3353–61.
[36] Zeeman R, Dijkstra PJ, van Wachem PB, van Luyn MJ, Hendriks M, Cahalan PT, et al. Successive epoxy and carbodiimide crosslinking of dermal sheep collagen. Biomaterials 1999;20:921–31.
[37] Vizárová K, Bakos D, Rehákova M, Petríkova M, Panáková E, Koller J. Modification of layered atelocollagen: enzymatic degradation and cytotoxicity evaluation. Biomaterials 1995;16: 1217–21.
[38] Park S-N, Park J-C, Kim HO, Song MJ, Suh H. Characterization of porous collagen/hyaluronic acid scaffold modified by 1-ethyl-3-(3-dimethylaminopropyl)carbodiimide cross-linking. Biomaterials 2002;23:1205–12.
[39] Ma L, Gao C, Mao Z, Zhou J, Shen J. Enhanced biological stability of collagen porous scaffolds by using amino acids as novel cross-linking bridges. Biomaterials 2004;25:2997–3004.

J Artif Organs (2007) 10:104–108
DOI 10.1007/s10047-006-0367-7

ORIGINAL ARTICLE

Tsuyoshi Kimura, PhD · Sayaka Iwai
Toshiyuki Moritan, PhD · Kwangwoo Nam, PhD
Shingo Mutsuo · Hidekazu Yoshizawa, PhD
Masahiro Okada, PhD · Tsutomu Furuzono, PhD
Tosihya Fujisato, PhD · Akio Kishida, PhD

Preparation of poly(vinyl alcohol)/DNA hydrogels via hydrogen bonds formed on ultra-high pressurization and controlled release of DNA from the hydrogels for gene delivery

Abstract Poly(vinyl alcohol) (PVA) hydrogels interacting with DNA mediated by hydrogen bonds (PVA/DNA hydrogel) were developed using ultra-high pressure (UHP) technology. The goal was to create a new method of gene delivery by controlled release of DNA. Mixed solutions of DNA and PVA at various concentrations were pressurized at 10000 atmospheres at 37°C for 10min. PVA/DNA hydrogels with good formability were produced at PVA concentrations of more than 5% w/v. The presence of DNA in the obtained hydrogels was confirmed by spectroscopic analysis and nucleic acid dye staining. DNA release from the hydrogels was investigated using PVA/DNA hydrogel samples of 5% and 10% w/v formed by UHP treatment or by conventional freeze–thaw methods. The DNA release curves from both types of samples showed a rapid phase in the initial 15h followed by a sustained release phase. However, there was a difference in the amount of DNA released. Less DNA was released by the pressurized hydrogels than by the freeze–thaw hydrogels. Also, the cumulative amount of DNA released decreased as the PVA content in the hydrogels increased. These results indicate that DNA release from the hydrogels can be modulated by changing the preparation method and the PVA content. Furthermore, it was demonstrated that DNA release could be controlled by varying the amount and duration of pressurizing used to form the hydrogels. Intact fractions of plasmid DNA released from the hydrogels were separated by agarose gel electrophoretic analysis. These results suggest that, using controlled release, DNA from PVA/DNA hydrogels formed by UHP treatment can be transfected into cells.

Key words Controlled release · Ultra-high pressure · DNA · Hydrogel · Poly(vinyl alcohol)

Received: March 31, 2006 / Accepted: November 18, 2006

T. Kimura · K. Nam · A. Kishida (✉)
Institute of Biomaterials and Bioengineering, Tokyo Medical and Dental University, 2-3-10 Kanda-Surugadai, Chiyoda-ku, Tokyo 101-0062, Japan
Tel. and Fax +81-3-5280-8028
e-mail: kishida.fm@tmd.ac.jp

S. Iwai · T. Moritan
Department of Medical Engineering, Suzuka University of Medical Science, Suzuka, Japan

S. Mutsuo · H. Yoshizawa
Department of Environmental Chemistry and Materials, Okayama University, Okayama, Japan

M. Okada · T. Furuzono
Department of Biomedical Engineering, National Cardiovascular Center Research Institute, Osaka, Japan

T. Fujisato
Department of Regenerative Medicine and Tissue Engineering, National Cardiovascular Center Research Institute, Osaka, Japan

Introduction

Safe and biocompatible synthetic materials have been developed as biomaterials.[1] In gene therapy, nonviral synthetic gene carriers have been the focus of attention due to their biological safety advantages over viruses.[2] In many cases, cationic synthetic materials, such as cationic lipids, liposomes,[3] polyethyleneimine,[4] polyamideamine dendrimer,[5] poly-L-lysine (PLL), PLL derivatives,[6] and other cationic peptides,[7] have been used as nonviral vectors. It is possible to form complexes between these materials and DNA using the electrostatic interaction between their cationic groups and the anionic groups of DNA, making the DNA robust against nuclease degradation and enabling effective transfection into mammalian cells.[8,9] However, the cytotoxicity of cationic materials was reported to be a significant problem.[10,11] For safer and more efficient gene delivery, it is necessary to develop a noncationic or less cationic gene carrier through nonelectrostatic interaction with DNA. Sakurai et al. reported that a triple helical complex of single-strand DNA and double-strand schizophyllan, which is a kind of polysaccharide (β-1,3 glucan), was formed through hydrogen bonding.[12] In addition, we previously reported that nanoparticles of poly(vinyl alcohol) (PVA) bonded to DNA via hydrogen bonds were obtained when mixed solutions of PVA (less than 0.01% w/v) and DNA were treated under ultra-high pressure (UHP) at

10000 atmospheres (980MPa) and 40°C for 10min.[13] It is well known that intra- and intermolecular hydrogen bonding increases in these conditions.[14] The PVA/DNA nanoparticles could be internalized into mammalian cells, suggesting that they have utility as a novel nonviral vector that uses nonelectronic interactions.

Recently, controlled release of DNA was also investigated as a possible method of enhancing transfection efficiency using various biomaterials such as poly (lactide-co-glycolide) (PLGA),[15] hyaluronic acid,[16] atelocollagen,[17] and gelatin.[18,19] Shea et al. reported that the sustained delivery of DNA from PLGA led to effective transfection of a large number of cells in vitro and in vivo.[15] However, it was difficult to regulate the release of DNA owing to the lack of interaction forces, such as covalent, electrostatic, and hydrogen bonding, with which DNA molecules are loaded into PLGA with polymer molecules. Tabata et al. reported enhancement and prolongation of gene expression using a cationized gelatin hydrogel interacting with DNA electrostatically.[18,19] The controlled release of DNA depended on hydrogel degradation, but the cationized gelatin hydrogel was crosslinked by glutaraldehyde, which has generally cytotoxic properties, to obtain different degrees of cationization.

In the present study, we report the preparation of a novel PVA hydrogel with DNA crosslinked physically by hydrogen bonds using UHP technology and its application to the controlled release of DNA. The goal is to develop an effective, low-cytotoxic and gene-releasable biomaterial. PVA/DNA hydrogels were obtained for various pressurization conditions, temperatures, and processing times. DNA release from the hydrogels was investigated in vitro. PVA is widely used for biomedical applications because of its biocompatibility and neutrally charged nature.[20] It is also known that PVA hydrogel is formed by physical crosslinking with hydrogen bonds when PVA solution is frozen and thawed several times, which is called the freeze–thaw method.[21]

Materials and methods

Materials

In our experiments, we used PVA samples with an average molecular weight of 74800 and a degree of saponification of 99.8%, as supplied by Kuraray (Osaka, Japan). We also used salmon sperm DNA purchased from Wako (Osaka, Japan), plasmid DNA encoding enhanced green fluorescence protein under a cytomegalovirus promoter (pEGFP-N1, BD Science, Palo Alto, CA, USA), and nucleic acid staining dye solution (Mupid Blue) obtained from Advance (Tokyo, Japan).

Preparation of PVA/DNA hydrogels by UHP

Aqueous PVA solutions of 6%, 8%, 10%, 14%, and 20% w/v were prepared by autoclaving three times for 30min at 121°C. Salmon sperm DNA was dissolved in a Tris-EDTA buffer (TE, pH = 7.8) at a concentration of 16.3mg/ml. The DNA solution was mixed with PVA solutions of 10%, 14%, and 20% w/v at a ratio of 1:1. The 0.7-ml samples were transferred in silicon tubes (9 × 25mm) with both ends capped by silicon plugs. The tubes were pressurized under various UHP conditions, using different pressures, temperatures, and durations, in a high-pressure machine (Kobe Steel, Kobe, Japan).

Confirmation of the presence of DNA in the PVA/DNA hydrogels

The presence of DNA in the PVA/DNA hydrogels produced by UHP treatment was confirmed by nucleic acid dye staining and UV-visible spectroscopy. For the former method, the PVA/DNA hydrogels were immersed in nucleic acid dye solution for 1min and then transferred to 70% ethanol. After 1min, they were immersed in ion-exchanged water for 1min. For the latter method, after the PVA/DNA hydrogels were melted at 90°C for 10min, their DNA concentration was measured by a spectrophotometer (V-560, JASC, Tokyo, Japan).

DNA release from hydrogels

The PVA/DNA hydrogels prepared by UHP were immersed in 5ml of phosphate-buffered saline (PBS) for 144h at 37°C. At 0.25, 0.5, 2, 3, 15, 27, 48, 111, and 144h, 20μl of the samples in the outer part of the PBS solution was collected and the DNA concentration was measured spectrophotometrically at 260nm (Gene Quant Pro S, Amersham, Tokyo, Japan).

Stability of plasmid DNA released from hydrogels

Plasmid DNA (pDNA) was used instead of salmon sperm DNA and the mixed solutions of pDNA (100μg/ml) and PVA (5% or 10% w/v) were treated by UHP under the conditions described above. The obtained PVA/pDNA hydrogels were immersed in PBS for 12 and 48h, and then the samples in the outer part of the solution were collected and analyzed by agarose gel electrophoresis at 100V for 45min.

Results and discussion

Aqueous solutions of PVA at concentrations ranging from 3% to 10% w/v were hydrostatically pressurized at 10000atm at 37°C for 10min. With a PVA solution of 3% w/v, the clear solution was transformed into a turbid and viscous solution by pressurization (Fig. 1A). An aggregation of PVA particles with an average diameter of 1μm was observed in the PVA solution on scanning electron microscopy (SEM, data not shown). For PVA concentrations of more than 4% w/v, hydrogels were produced on pressuriza-

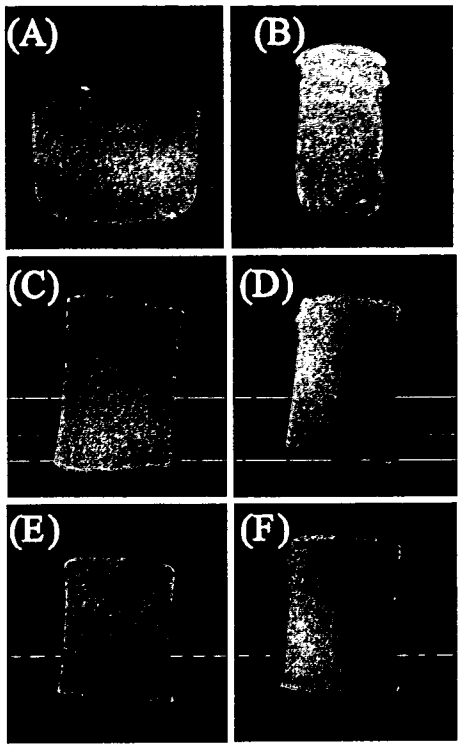

Fig. 1. Photographs of poly(vinyl alcohol) (PVA) hydrogels (**A–D**) and PVA/DNA (**E,F**) hydrogels at concentrations of **A** 3% w/v, **B** 4% w/v, **C,E** 5% w/v, and **D,F** 10% w/v obtained by ultra-high pressure treatment

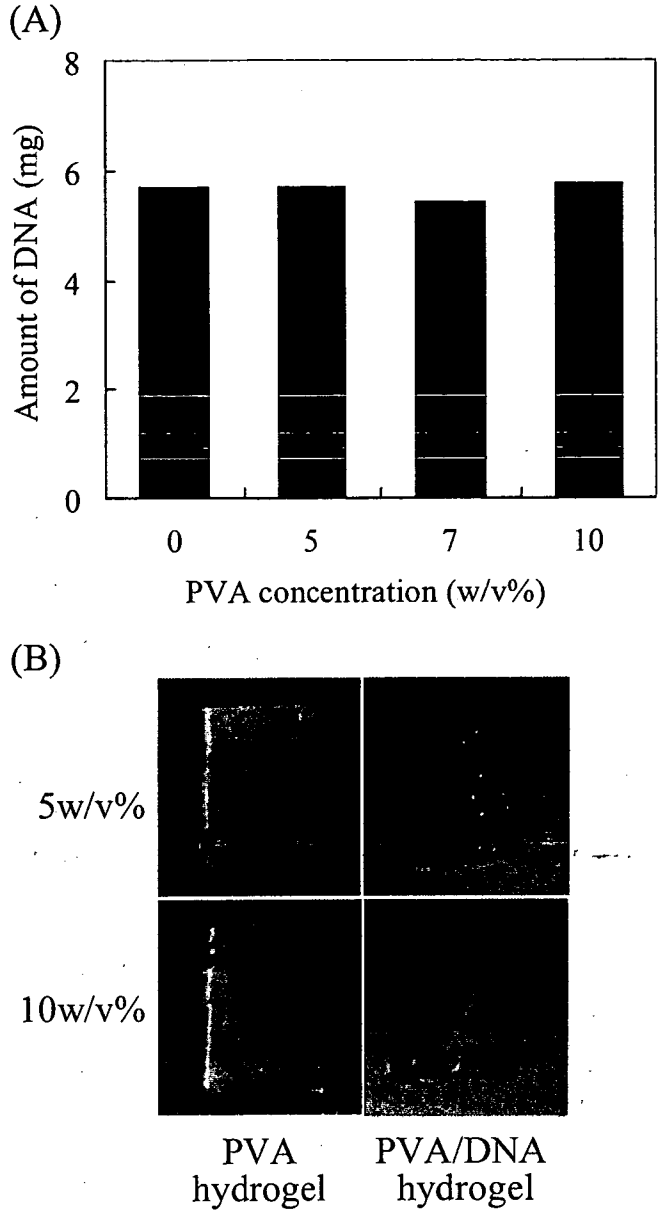

Fig. 2A,B. Presence of DNA in PVA/DNA hydrogels. **A** Amount of DNA in solution obtained by melting PVA/DNA hydrogels prepared using ultra-high pressure processing. **B** Photographs of PVA hydrogels and PVA/DNA hydrogels stained with nucleic acid dye

tion (Fig. 1B–D). The PVA hydrogel of 4% w/v was fragile (Fig. 1B), but increasing the PVA concentration enhanced hydrogel formability, and hard hydrogels were obtained at a PVA concentration of 10% w/v (Fig. 1D). These results indicate that pressurization induced physical cross-linking of PVA molecules and that the degree of cross-linking increased as the PVA concentration increased. To investigate whether the PVA molecules were physically cross-linked by hydrogen bonding, a PVA solution of 5% w/v with urea (3.3M), which was used as a hydrogen bond inhibitor, was treated under the above pressurizing conditions. The solution remained translucent (data not shown), indicating that the PVA hydrogel obtained by pressurization was mediated by hydrogen bonding.

The gelation of mixed solutions of DNA and PVA (5% and 10% w/v) was achieved by pressurization in the conditions described above (Fig. 1E,F). To confirm the presence of DNA in the hydrogels obtained, they were heat treated at 90°C for 10min and then the DNA concentration of the solutions obtained was measured spectrophotometrically at 260nm. Roughly equal amounts of DNA were contained in each hydrogel (Fig. 2A). Also, when the hydrogels were immersed in nucleic acid dye solution, which interacts electrostatically with the phosphate groups of DNA, the PVA hydrogel with DNA was stained, whereas the PVA hydrogel without DNA was not (Fig. 2B). These results indicate that a PVA hydrogel that sustains DNA (PVA/DNA hydrogel) was formed on pressurization. On the other hand, when urea was introduced, PVA/DNA hydrogel was not obtained on pressure treatment. This result suggests that hydrogen bonding between PVA and DNA took place in the pressurized PVA/DNA hydrogel.

DNA release from the PVA/DNA hydrogel formed by pressurization at 10000atm at 37°C for 10min was investigated. PVA/DNA hydrogels produced by the freeze–thaw method, a common method of forming PVA hydrogels,[21] were used as control samples. Figure 3A shows DNA release profiles from the PVA/DNA hydrogels at PVA concentrations of 5% and 10% w/v obtained by pressurization and the freeze–thaw method. Each release curve of DNA from a hydrogel consisted of a rapid phase in the initial 15h followed by a sustained release phase. However, the amount

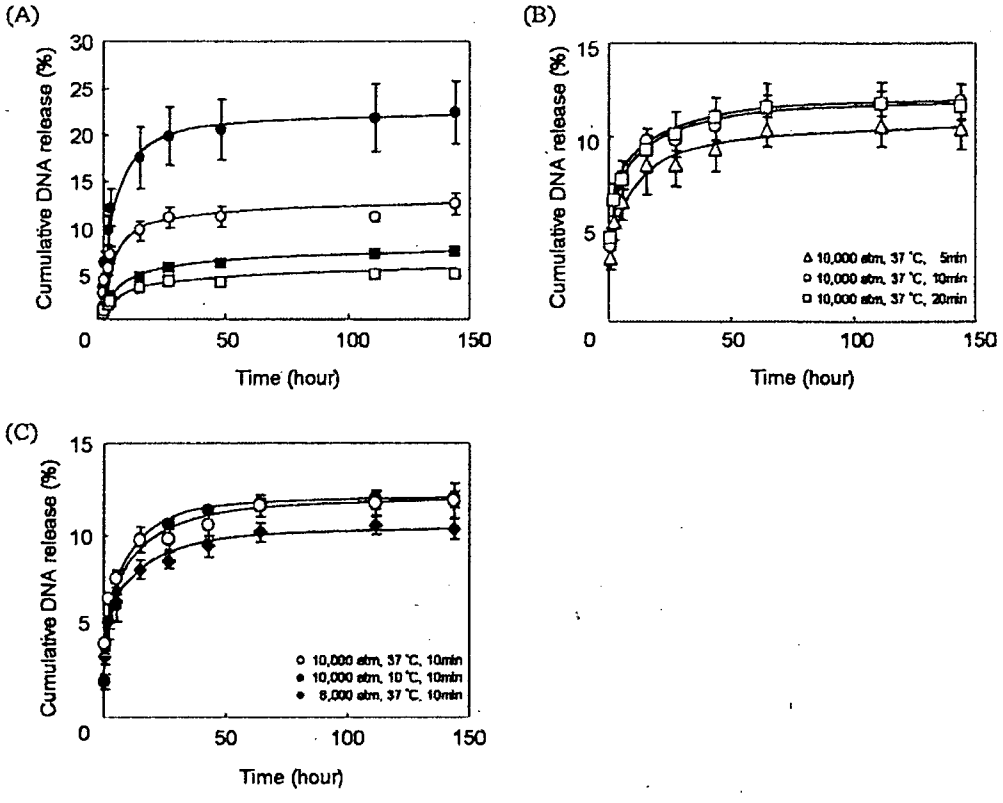

Fig. 3A–C. DNA release test from PVA/DNA hydrogels produced by pressurization under various conditions or by the freeze–thaw method. **A** Release profiles of DNA from hydrogels at PVA concentrations of 5% w/v (○, ●) and 10% w/v (□, ■) PVA concentration. *Open* and *solid* symbols indicate DNA from hydrogels obtained by pressurization (at 10000 atm and 37°C, 10 min) and the freeze–thaw method, respectively. **B** Release profiles of DNA from hydrogels of 5% w/v obtained by pressurization at 10000 atm and 37°C for 5 min (□), 10 min (○), and 20 min (□). **C** Release profiles of DNA from hydrogels of 5% w/v obtained by pressurization at 10000 atm and 37°C (○), 10000 atm and 10°C (●), and 8000 atm and 37°C (□) for 10 min

of DNA released was dependent on PVA content and on which procedure was used to prepare the hydrogels. The DNA release from the 10% w/v PVA/DNA hydrogels was lower than that from the 5% w/v PVA/DNA hydrogels, irrespective of the preparation methods. This is consistent with the fact that the 5% w/v samples were more easily stained by nucleic acid dye than the 10% w/v samples. We suppose that the increased crosslinking in the hydrogel caused by the increase in the PVA content contributed to the reduction of DNA released from the hydrogel. On the other hand, at the same PVA concentrations, DNA was more effectively released from the freeze–thaw hydrogels than from the pressurized hydrogels. Fibrous structures with large spaces (larger than 1 μm) were observed on SEM in the hydrogels made from 5% w/v PVA obtained by the freeze–thaw method, while many porous structures with diameters of 300 μm were observed in the pressurized hydrogels (data not shown). We believe that this difference in internal structure between sample types affected the interaction of PVA and DNA, resulting in the larger release of DNA from the freeze–thaw hydrogels.

To investigate the influence of the pressure conditions used to form hydrogels on DNA release, PVA/DNA hydrogels of 5% w/v were prepared by different levels of pressurization at different temperatures and for different durations. First, with pressure processing periods varying from 5 to 20 min at 10000 atm and 37°C, similar DNA release profiles were exhibited for the hydrogels obtained at pressurizing times of 10 and 20 min, but the amount of DNA released by hydrogel samples pressurized for 5 min (Fig. 3B) was less than that released by samples with longer pressurizing times. Second, the DNA release curves of the PVA/DNA hydrogel produced on pressurization at 10000 atm and 10°C for 10 min were the same as those for hydrogels produced on pressurization at 10000 atm and 37°C for 10 min. However, less DNA was released by hydrogels produced at pressures of 8000 atm and 37°C for 10 min than by hydrogels produced at 10000 atm and 37°C for 10 min (Fig. 3C). These results indicate that DNA release from pressurized hydrogels is dependent on the level and duration of pressure used in the hydrogel formation process. We previously reported that PVA gelation was promoted by increasing the pressure and by prolonging the pressurization time, by which close hydrogen bonds between PVA molecules are formed.[22] It seems that DNA was easily released from PVA/DNA hydrogels pressurized under conditions of more than 10000 atm for longer than 10 min because the hydrogen bonding interaction between PVA and DNA was more unstable than that between PVA molecules under more intense pressure conditions.

It is important for DNA to be released from hydrogels without structural change or degradation.[2,23] Plasmid DNA (pDNA), which is generally used as the DNA delivered by a nonviral vector, was used instead of salmon sperm DNA. PVA/pDNA hydrogels at PVA concentrations of 5% and 10% w/v were obtained by pressurization at 10000 atm at 37°C for 10 min and then immersed in 5 ml PBS. After 12 and 48 h of immersion, the outer part of the solution was collected and analyzed by agarose gel electrophoresis at 100 V for 30 min to investigate the stability of released pDNA from the hydrogels (Fig. 4). No degradation of DNA was observed, indicating that the plasmid DNA released

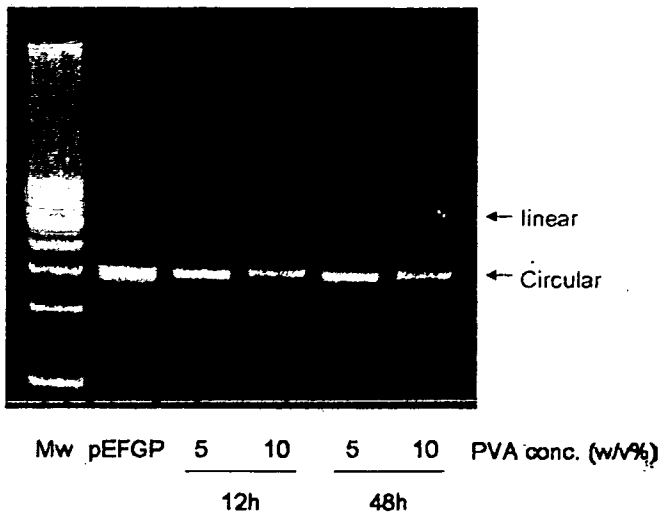

Fig. 4. Agarose gel electrophoresis of plasmid DNA (pDNA) released from PVA/pDNA hydrogels with PVA concentrations of 5% and 10% w/v produced by pressurization at 10000 atm and 37°C for 10 min after immersion in phosphate-buffered saline for 12 and 48 h

from the PVA/DNA hydrogels was stable. Two bands of linear and circular plasmid DNA were observed with 5% w/v PVA/DNA hydrogel, while circular plasmid DNA was released from the 10% w/v PVA/DNA hydrogel, indicating that the linear form of plasmid DNA tends to interact more strongly with PVA than the circular plasmid DNA.

Conclusions

Novel PVA/DNA hydrogels crosslinked physically by hydrogen bonds were developed using UHP technology. DNA released from the hydrogels was controlled by varying the PVA concentration and pressurization conditions, such as the level and duration of pressure used to form the hydrogels. The demonstrated stability of the DNA released from the hydrogels suggests that PVA/DNA hydrogels have potential as a candidate for gene delivery.

Acknowledgments This work was supported by grants from the Ministry of Health, Labor and Welfare, of Japan and the Ministry of Education, Culture, Sports, Science and Technology of Japan. We thank Kuraray, Co., Ltd., for supplying the poly(vinyl alcohol).

References

1. Nowak T, Nishida K, Shimoda S, Konno Y, Ichinose K, Sakakibara M, Shichiri M, Nakabayashi N, Ishihara K. Biocompatiblility of MPC: in vivo evaluation for clinical application. J Artif Organs 2000;1:39–46
2. Glover DJ, Lipps HJ, Jans DA. Towards safe, non-viral therapeutic gene expression in humans. Nat Rev Genet 2005;6:299–310
3. Zhang S, Xu Y, Wan B, Qiao W, Liu D, Li Z. Cationic compounds used in lipoplexes and polyplexes for gene delivery. J Control Release 2004;100:165–180
4. Lungwitz U, Breunig M, Blunk T, Göpferich A. Polyethylenimine-based non-viral gene delivery systems. Eur J Pharm Biopharm 2005;60:247–266
5. Dufes C, Uchegbu IF, Scatzlein AG. Dendrimers in gene delivery. Adv Drug Deliv Rev 2005;57:2117–2202
6. Kimura T, Yamaoka T, Iwase R, Murakami A. Effect of physicochemical properties of polyplexes composed of chemically modified PL derivatives on transfection efficiency in vitro. Macromol Biosci 2002;2:437–446
7. Futaki S. Membrane-permeable arginine-rich peptides and the translocation mechanisms. Adv Drug Deliv Rev 2005;57:547–558
8. Reschel T, Koňák C, Oupický D, Seymour LW, Ulbrich K. Physical properties and in vitro transfection efficiency of gene delivery vectors based on complexes of DNA with synthetic polycations. J Control Release 2002;81:201–217
9. Elouahabi A, Ruysschaert JM. Formation and intracellular trafficking of lipoplexes and polyplexes. Mol Ther 2005;11:336–347
10. Fischer D, Li Y, Ahlemeyer B, Krieglstein J, Kissel T. In vitro cytotoxicity testing of polycations: influence of polymer structure on cell viability and hemolysis. Biomaterals 2006;24:1121–1131
11. Choksakulnimitr S, Matsuda S, Tokuda H, Takakura Y, Hashida M. In vitro cytotoxicity of macromolecules in different cell culture systems. J Control Release 1995;34:233–241
12. Sakurai K, Mizu M, Shinkai S. Polysaccharide–polynucleotide complexes. 2. Complementary polynucleotide mimic behavior of the natural polysaccharide schizophyllan in the macromolecular complex with single-stranded RNA and DNA. Biomacromolecules 2001;2:641–650
13. Kimura T, Okuno A, Miyazaki K, Furuzono T, Ohya Y, Ouchi T, Mutsuo S, Yoshizawa H, Kitamura Y, Fujisato T, Kishida A. Novel PVA-DNA nonoparticles prepared by ultra high pressure technology for gene delivery. Mater Sci Eng C 2004;24:797–801
14. Doi E, Shimizu A, Kitabatake N. Gel-sol transition of ovalbumin by high pressure. In: Hayashi R (ed) High pressure bioscience and food science. Kyoto: Sanei Press, 1993;171–177
15. Shea LD, Smiley E, Bonadio J, Mooney DJ. DNA delivery from polymer matrices for tissue engineering. Nat Biotech 1999;17: 551–554
16. Chun KW, Lee JB, Kim SH, Rark TG. Controlled release of plasmid DNA from photo-cross-linked pluronic hydrogels. Biomaterials 2005;26:3319–3326
17. Ochiya T, Takahama Y, Nagahara S, Sumita Y, Hisada A, Itoh H, Nagai Y, Terada M. New delivery system for plasmid DNA in vivo using atelocollagen as a carrier material: the Minipellet. Nat Med 1999;5:707–710
18. Fukunaka Y, Iwanaga K, Morimoto K, Kakemi M, Tabata Y. Controlled release of plasmid DNA from cationized gelatin hydrogels based on hydrogel degradation. Biomaterials 2005;26:3319–3326
19. Kushibiki T, Tomoshige R, Fukunaka Y, Kakemi M, Tabata Y. In vivo release and gene expression of plasmid DNA by hydrogels of gelatin with different cationization extents. J Control Release 2003;90:207–216
20. Miyashita H, Shimmura S, Kobayashi H, Taguchi T, Asano-Kato K, Uchino Y, Kato M, Shimazaki J, Tanaka J, Tsubota K. Collagen-immobilized poly (vinyl alcohol) as an artificial cornea scaffold that supports a stratified corneal epithelium. J Biomed Mater Res Part B: Appl Biomater 2006;76B:56–63
21. Hyon SH, Cha WI, Ikada Y. Preparation of transparent poly (vinyl alcohol) hydrogel. Polymer Bull 1989;22:119–122
22. Yamamoto K, Furuzono T, Kishida A, Mustuo S, Yoshizawa H, Kitamura Y. Formation of a supramolecular assembly of poly (vinyl alcohol) by ultrahigh pressure. Meeting Report of the Poval Committee 2002;121:25–26
23. Walter E, Moelling K, Pavolvich HP. Microencapsulation of DNA using poly (D,L-lactide-co-glycolide): stability issues and release characteristics. J Control Release 1999;61:361–374